

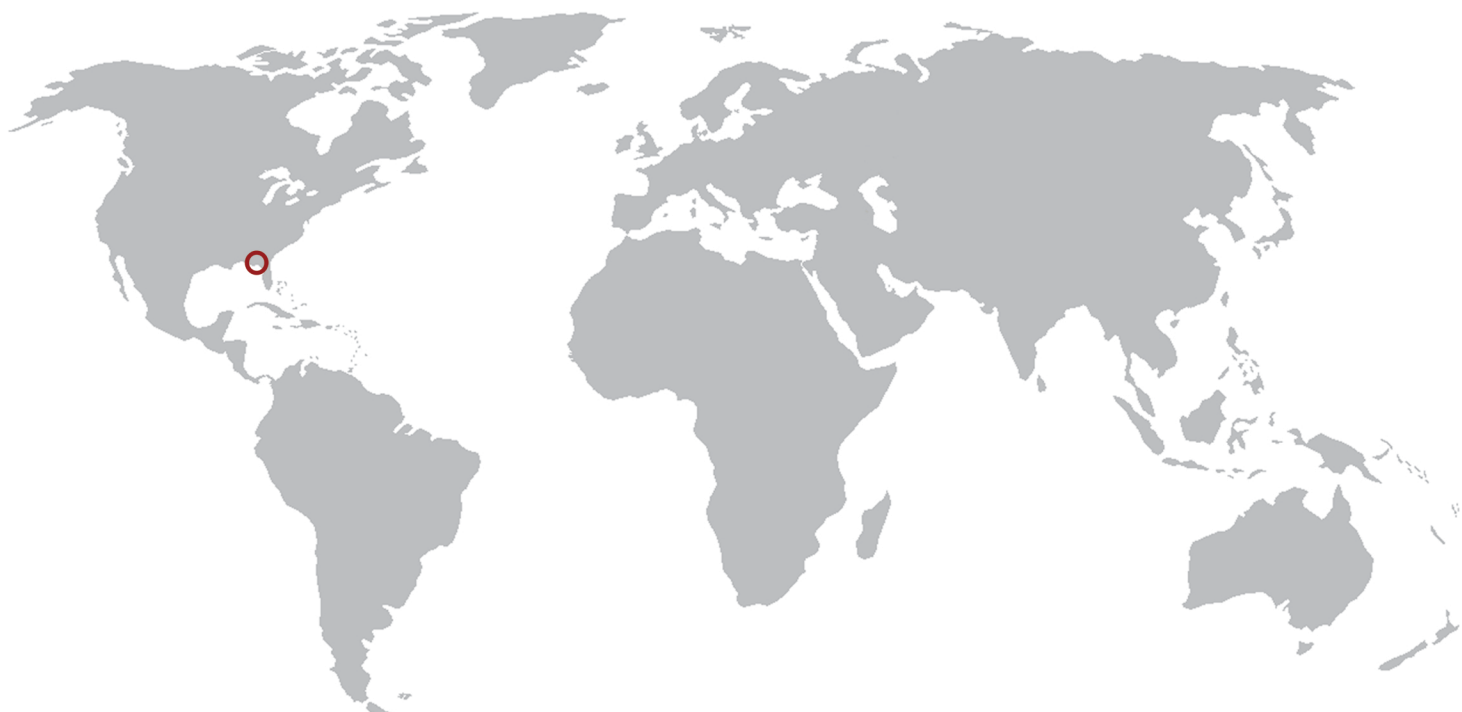
P R O C E E D I N G S

MMM 2008
Fourth
International Conference

MULTISCALE MATERIALS MODELING

OCTOBER 27-31, 2008 • TALLAHASSEE, FLORIDA, USA

*Tackling Materials Complexities
via Computational Science*



Hosted by the Department of Scientific Computing and Florida State University

DEPARTMENT OF
Scientific
COMPUTING



Proceedings of

MMM 2008
*Fourth
International Conference*
MULTISCALE MATERIALS MODELING
OCTOBER 27-31, 2008 • TALLAHASSEE, FLORIDA, USA

Anter El-Azab
Editor

**Organized and Hosted by
The Department of Scientific Computing and
Florida State University**

DEPARTMENT OF
Scientific
COMPUTING



Papers published in this volume constitute the proceedings of the Fourth International Conference on Multiscale Materials Modeling (MMM-2008). Papers were selected by the program committee for oral or poster presentation. They are published as submitted, in the interest of timely dissemination.

ISBN 978-0-615-24781-6

Copyright © 2008
Department of Scientific Computing
Florida State University
400 Dirac Science Library
P.O. Box 3064120
Tallahassee, FL 32306-4120

All rights reserved. No part of this publication may be translated, reproduced, stored in a retrieval system, or transmitted in any form or by any means, electronic, mechanical, photocopying, recording or otherwise, without the written permission of the publisher.

Printed in the United States of America

Forward

The field of multiscale modeling of materials promotes the development of predictive materials research tools that can be used to understand the structure and properties of materials at all scales and help us process materials with novel properties. By its very nature, this field transcends the boundaries between materials science, mechanics, and physics and chemistry of materials. The increasing interest in this field by mathematicians and computational scientists is creating opportunities for solving computational problems in the field with unprecedented levels of rigor and accuracy. Because it is a part of the wider field of materials science, multiscale materials research is intimately linked with experiments and, together, these methodologies serve the dual role of enhancing our fundamental understanding of materials and enabling materials design for improved performance.

The increasing role of multiscale modeling in materials research motivated the materials science community to start the Multiscale Materials Modeling (MMM) Conference series in 2002, with the goal of promoting new concepts in the field and fostering technical exchange within the community. Three successful conferences in this series have been already held:

- The First International Conference on Multiscale Materials Modeling (MMM-2002) at Queen Mary University of London, UK, June 17-20, 2002,
- Second International Conference on Multiscale Materials Modeling (MMM-2004) at the University of California in Los Angeles, USA, October 11-15, 2004, and
- Third International Conference on Multiscale Materials Modeling (MMM-2006) at the University of Freiburg, Germany, September 18-22, 2006.

The Fourth International Conference on Multiscale Materials Modeling (MMM-2008) held at Florida State University comes at a time when the wider computational science field is shaping up and the synergy between the materials modeling community and computational scientists and mathematicians is becoming significant. The overarching theme of the MMM-2008 conference is thus chosen to be “*Tackling Materials Complexities via Computational Science*,” a theme that highlights the connection between multiscale materials modeling and the wider computational science field and also reflects the level of maturity that the field of multiscale materials research has come to. The conference covers topics ranging from basic multiscale modeling principles all the way to computational materials design. Nine symposia have been organized, which span the following topical areas:

- Mathematical basis for multiscale modeling of materials
- Statistical frameworks for multiscale materials modeling
- Mechanics of materials across time and length scales
- Multiscale modeling of microstructure evolution in materials
- Defects in materials
- Computational materials design based on multiscale and multi-level modeling principles

- Multiscale modeling of radiation effects in materials and materials response under extreme conditions
- Multiscale modeling of bio and soft matter systems

The first five topical areas are intended to cover the theoretical and computational basis for multiscale modeling of materials. The sixth topical area is intended to demonstrate the technological importance and industrial potential of multiscale materials modeling techniques, and to stimulate academia-laboratory-industrial interactions. The last two topical areas highly overlap with the earlier ones, yet they bring to the conference distinct materials phenomena and modeling problems and approaches with unique multiscale modeling aspects.

This conference would not have been possible without the help of many individuals both at Florida State University and around the world. Of those, I would like to thank the organizing team of MMM-2006, especially Professor Peter Gumbsch, for sharing their experience and much organizational material with us. I also thank all members of the International Advisory Board for their support and insight during the early organizational phase of the conference, and the members of the International Organizing Committee for the hard work in pulling the conference symposia together and for putting up with the many organization-related requests. Thanks are due to Professor Max Gunzburger, Chairman of the Department of Scientific Computing (formerly School of Computational Science) and to Florida State University for making available financial, logistical and administrative support without which the MMM-2008 would not have been possible. The following local organizing team members have devoted significant effort and time to MMM-2008 organization: Bill Burgess, Anne Johnson, Michele Locke, Jim Wilgenbusch, Christopher Cprek and Michael McDonald. Thanks are also due to my students Srujan Rokkam, Steve Henke, Jie Deng, Santosh Dubey, Mamdouh Mohamed and Jennifer Murray for helping with various organizational tasks. Special thanks are due to Bill Burgess and Srujan Rokkam for their hard work on the preparation of the proceedings volume and conference program.

I would like to thank the MMM-2008 sponsors: Lawrence Livermore National Laboratory (Dr. Tomas Diaz de la Rubia), Oak Ridge National Laboratory (Dr. Steve Zinkle) and Army Research Office (Drs. Bruce LaMattina and A.M. Rajendran) for the generous financial support, and thank TMS (Dr. Todd Osman) for the sponsorship of MMM-2008 and for advertising the conference through the TMS website and other TMS forums.

I would also like to thank all plenary speakers and panelists for accepting our invitation to give plenary lectures and/or serve on the conference panels. Lastly, I would like to thank the session chairs for managing the conference sessions.

Anter El-Azab
Conference Chair

International Advisory Board

Dr. Tomas Diaz de la Rubia	LLNL, USA
Prof. Peter Gumbsch	Fraunhofer Institute IWM, Freiburg, Germany
Dr. A.M. Rajendran	ARO, USA
Dr. Steve Zinkle	ORNL, USA
Prof. Anter El-Azab	FSU, USA
Prof. Michael Zaiser	Edinburgh, UK
Prof. Xiao Guo	Queens, London, UK
Prof. Shuichi Iwata	University of Tokyo, Japan
Prof. Jan Kratochvil	CTU, Prague, Czech Republic
Prof. Nasr Ghoniem (Chair)	UCLA, USA
Dr. Ladislav Kubin	ONERA-LEM, France
Prof. Shaker Meguid	Toronto, Canada
Prof. Alan Needleman	Brown, USA
Prof. Michael Ortiz	Caltech, USA
Prof. David Pettifor	Oxford, UK
Prof. Robert Phillips	Caltech, USA
Prof. Dierk Raabe	Max Planck Institute, Duesseldorf, Germany
Prof. Yoji Shibutani	Osaka University, Japan
Prof. Subra Suresh	MIT, Massachusetts USA
Prof. Yoshihiro Tomita	Kobe University, Japan
Prof. Erik Van der Giessen	University of Groningen, The Netherlands
Dr. Dieter Wolf	INL, USA
Prof. Sidney Yip	MIT, USA
Prof. David Bacon	Liverpool, UK
Dr. Michael Baskes	LANL, USA
Prof. Esteban Busso	Ecole des Mines, France
Prof. Timothy Cale	RPI, New York, USA
Dr. Moe Khaleel	PNNL, USA
Prof. David Srolovitz	Yeshiva, USA
Prof. Emily Carter	Priceton University, USA
Dr. Dennis Dimiduk	AFRL, USA
Prof. Rich Le Sar	Iowa State University, USA

International Organizing Committee

Weinan E	Princeton University, USA
Max Gunzburger	Florida State University, USA
Mitchell Luskin	University of Minnesota, USA
Rich Lehoucq	Sandia National Laboratories, USA
A.M. Rajendran	U.S. Army Research Office, USA
Stefano Zapperi	University of Rome, Italy
M.-Carmen Miguel	University of Barcelona, Spain
Mikko Alava	Helsinki University of Technology, Finland
Istevan Groma	Eötvös University, Hungary
Tom Arsenlis	Lawrence Livermore National Laboratory, USA
Peter Chung	Army Research Laboratory, USA

Marc Geers	Eindhoven University of Technology, The Netherlands
Yoji Shibutani	Osaka University, Japan
Dieter Wolf	Idaho National Laboratory, USA
Jeff Simmons	Air Force Research Laboratory, USA
Simon Phillpot	University of Florida, USA
Anter El-Azab (Chair)	Florida State University, USA
Daniel Weygand	University of Karlsruhe (TH), Germany
Zi-Kui Liu	Pennsylvania State University, USA
Hamid Garmestani	Georgia Institute of Technology, USA
Moe Khaleel	Pacific Northwest National Laboratory, USA
Mei Li	Ford Motor Company, USA
Fie Gao	Pacific Northwest National Laboratory, USA
Roger Stoller	Oak Ridge National Laboratory, USA
Pascal Bellon	University of Illinois, Urbana-Champaign, USA
Syo Matsumura	Kyushu University, Japan
Jeffery G. Saven	University of Pennsylvania, USA
Wei Yang	Florida State University, USA
T.P. Straatsma	Pacific Northwest National Laboratory, USA
L.P. Kubin	CNRS-ONERA, France
S.J. Zinkle	Oak Ridge National Laboratory, USA
Jaafar El-Awady	University of California, Los Angeles, USA
Shahram Sharafat	University of California, Los Angeles, USA
Hanchen Huang	Rensselaer Polytechnic Institute, USA
Yury N. Osetskiy	Oak Ridge National Laboratory, USA
Ron O. Scattergood	North Carolina State University, USA
Anna M. Serra	Universitat Politècnica de Catalunya, Spain

Local Organizing Committee (Florida State University, USA)

Prof. Anter El-Azab (Chair)
 Prof. Max Gunzburger (Co-Chair)
 Anne Johnson (Public relations and marketing)
 Bill Burgers (Graphics and publications)
 Srujan Rokkam (Proceedings and printing)
 Michael McDonald (Webmaster)
 Michele Locke (Finances)

Sponsors

Special thanks to the following sponsors:

- The Army Research Office
- Lawrence Livermore National Laboratory
- Oak Ridge National Laboratory

for their generous financial support, and to

- The Minerals, Metals & Materials Society (TMS)

for the sponsoring and advertising the conference through the TMS website.

Contents

Symposium 1

Multiscale Methods for Fluid and Plasma Dynamics R. Caflisch Session M-B	31
Kinetic Models for Dilute Polymers: Analysis, Approximation and Computation J. W. Barrett, D. Knezevic, E. Süli Session M-B	32
Coarse-graining of Macro-molecular Systems: Mathematical and Numerical Methods P. Plechac Session M-B	33
A Path-integral Formulation of DNA Looping Probabilities J. H. Maddocks, R. Manning, L. Cotta-Ramusino Session M-B	34
Mean Field Approximation of Transfer Operators in High-dimensional Conformation Dynamics G. Friesecke, O. Junge Session M-C	35
Some Recent Progress in Elliptic Homogenization X. Blanc, C. Le Bris, P.-L. Lions Session M-C	36
Micro-macro FENE Models for Polymeric Materials and their Closure Approximations Q. Du Session M-C	37
Homogenization with Nonseparated Scales L. Berlyand Session M-C	38
Toward Multiscale Modelling and Simulation of Fuel Cells I. Dabo, E. Cancès, Y. Li, N. Marzari Session M-D	39

Sub-linear Scaling Algorithms for the Study of the Electronic Structure of Materials C. J. Garcia-Cervera, J. Lu, W. E Session M-D	40
BOSSANOVA: A bond order dissection approach for efficient electronic structure calculations M. Griebel, J. Hamaekers, F. Heber Session M-D	41
Adaptive Control of Modeling Error for Multiscale Simulations J. T. Oden, S. Prudhomme, P. T. Bauman, L. Chamoin Session T-B	46
A New Frontier of Kinetic Theory Applications in Solid Mechanics—The Discrete-Continuum Connection in Dislocation Dynamics A. El-Azab Session T-B	47
Electronic Structure Calculations at Macroscopic Scales V. Gavini Session T-B	48
A Numerical Bridge Between Quantum and Molecular Dynamics based on the Ehrenfest Dynamics D. Aubry, A.-L. Hamon Session T-B	49
On a Stochastic Approach for Atomic-to-Continuum Coupling Methods L. Chamoin, S. Prudhomme, J. T. Oden, P. T. Bauman Session T-B	50
Mathematical Validation and Algorithms for the Quasicontinuum Method M. Luskin, M. Arndt, M. Dobson Session T-C	51
Comparing the Accuracy and Efficiency of Multiscale Methods R. E. Miller, E. B. Tadmor, M. Luskin Session T-C	52
1D Atomistic-to-Continuum Coupling via Optimization J. P. Reese, M. Gunzburger Session T-C	53

Approximating the quasicontinuum method using quadrature rules	57
Y. Zhang, M. Gunzburger Session T-C	
Analysis of Quasicontinuum Method	61
P. Ming Session W-B	
Quadrature and Implementation of the Weak Coupling Method	62
K. Fackeldey, D. Krause, R. Krause Session W-B	
Peridynamics, Molecular Dynamics, and Classical (nonlinear) Elasticity	66
R. Lehoucq, S. Silling Session W-B	
Molecular dynamics at Larger Scales: Peridynamics as an upscaling of molecular dynamics	67
M. L. Parks, P. Seleson Session W-B	
Coarse-graining the Free energy of Atomistic Systems: a simple case	68
X. Blanc, C. Le Bris, F. Legoll, C. Patz Session W-B	
Inverse Microstructure Design Based on Statistical correlation functions	69
H. Garmestani Session Th-B	
A Review of Recent Transition State Search Methods in Phase Transition Simulation	70
Y. Wang,, V. Lasrado, D. Alhat Session Th-B	
Finite Element Heterogeneous Multiscale Method and Micromagnetism	74
V. Melicher, J. Busa Session Th-B	
Homogenization of Stochastic Fractal Microstructures	75
R.C. Picu, M.A. Soare Session Th-B	

Finite Element Methods for a Peridynamic Model of Mechanics X. Chen, M. Gunzburger Session W-D	76
Bridging Methods and Boundary Treatment for AtC Coupling Problems P. Seleson, M. Gunzburger Session W-D	77
Effect of Thermal Cycling on Hardness of Plain Carbon Steel Abdlmanam Elmaryami Session W-D	81
Electronic Structure calculations of Novel Spinel Oxynitrides O. U. Okeke Session W-D	82
The Attainability of Hashin-Shtrikman Bounds L. Liu Session W-D	83
New Approach To Model Point Defects Migration Using A Monte-Carlo Paradigm Coupled With Artificial Intelligence N. Castin, L. Malerba Session W-D	87
Regression Possibilities of Isothermal Transformation (IT) and Continuous Cooling (CC) Transformation Diagrams using T-t Elements Z. Dudas Session W-D	91
Analytic Solution of the Discrete Double Sine-Gordon Model: application to crowdion migration in the bcc transition metals S. Fitzgerald, D. Nguyen-Manh, Z. Dudas Session W-D	92
Generalisation of the Diffusion-Reaction Theory for Inclusion Of Complexes with Long-Range Interaction Range A. V. Barashev, S. I. Golubov, D. J. Bacon, Y. N. Osetsky, R. E. Stoller Session W-D	93

Symposium 1

Mathematical issues in multiscale materials modeling

Multiscale Methods for Fluid and Plasma Dynamics

Russel Caflisch

**Department of Mathematics, University of California, Los Angeles, California
(E-mail: caflisch@math.ucla.edu)**

ABSTRACT

For small Knudsen number, simulation of rarefied gas dynamics (RGD) by particle methods (such as Direct Simulation Monte Carlo or DSMC) becomes computationally intractable because of the large collision rate. To overcome this problem we have developed a hybrid simulation method, combining DSMC and a fluid dynamic description. The molecular distribution function f is represented as a linear combination of a Maxwellian distribution M and a particle distribution g ; i.e., $f = bM + (1-b)g$. The density, velocity and temperature of M are governed by fluid-like equations, while the particle distribution g is simulated by DSMC. In addition there are interaction terms between M and g . The coefficient b is independent of velocity and represents the degree of thermalization. This method has been extended to simulation of Coulomb collisions in a plasma. Since the rate of Coulomb collisions is strongly dependent on velocity, the projection onto thermal component M and kinetic component g must be velocity dependent, for which we use thermalization and dethermalization probabilities that are functions of velocity. Numerical examples for both RGD and plasmas will be presented to illustrate the performance of the methods.

Kinetic Models for Dilute Polymers: Analysis, Approximation and Computation

John W. Barrett¹, David Knezevic², and Endre Süli²

¹Department of Mathematics, Imperial College London, London SW7 2AZ, UK.
(E-mail: j.barrett@imperial.ac.uk)

²Numerical Analysis Group, Oxford University Computing Laboratory, Wolfson Building, Parks Road, Oxford OX1 3QD, UK.
(E-mail: endre.suli@comlab.ox.ac.uk)

ABSTRACT

We review recent analytical [1,2,3] and computational results [4,5,6] for macroscopic-microscopic bead-spring models that arise from the kinetic theory of dilute solutions of incompressible polymeric fluids with noninteracting polymer chains, involving the coupling of the unsteady Navier-Stokes system in a bounded domain, in $d=2$ or 3 three space dimensions, with an elastic extra-stress tensor as right-hand side in the momentum equation, and a (possibly degenerate) Fokker-Planck equation over the $(2d+1)$ -dimensional region that is the cartesian product of the flow domain, the configuration space domain D and the time interval $[0,T]$. We consider the question of existence of global-in-time weak solutions to the model for a general class of spring potentials, including, in particular, the widely used finitely extensible nonlinear elastic (FENE) potential. The numerical approximation of this high-dimensional coupled system is a formidable computational challenge, complicated by the fact that for practically relevant spring potentials, such as the FENE potential, the drift term in the Fokker-Planck equation is unbounded on the boundary of D . We shall present numerical simulations for this coupled high-dimensional micro-macro model.

- [1] J.W. Barrett, C. Schwab and E. Süli, “Existence of Global Weak Solutions for Some Polymeric Flow Models”, *M3AS: Mathematical Models and Methods in Applied Sciences*, **6**, 939, 2005.
- [2] J.W. Barrett and E. Süli, “Existence of Global Weak Solutions to Some Regularized Kinetic Models of Dilute Polymers”, *SIAM Multiscale Modelling and Simulation*, **6**, 506, 2007.
- [3] J.W. Barrett and E. Süli, “Existence of Global Weak Solutions to Dumbbell Models for Dilute Polymers with Microscopic Cut-off”, *M3AS: Mathematical Models and Methods in Applied Sciences*, **18**, 935-971, 2008.
- [4] J.W. Barrett and E. Süli, “Numerical Approximation of Corotational Dumbbell Models for Dilute Polymers”, *IMA Journal of Numerical Analysis*, Accepted for publication, 19 March 2008. <http://web.comlab.ox.ac.uk/people/Endre.Suli/biblio.html>
- [5] J.W. Barrett and E. Süli, “Numerical Approximation of Kinetic Dilute Polymer Models with Microscopic Cut-off”, In preparation, 2008.
- [6] D. Knezevic and E. Süli, “Spectral Galerkin Approximation of Fokker-Planck Equations with Unbounded Drift”, *M2AN*, Submitted for publication, February 2008. <http://web.comlab.ox.ac.uk/people/Endre.Suli/biblio.html>

Coarse-graining of Macro-molecular Systems: Mathematical and Numerical Methods

Petr Plechac

**Department of Mathematics, University of Tennessee, Knoxville, Tennessee
(E-mail: plechac@math.utk.edu)**

ABSTRACT

We present mathematical tools developed for error control in microscopic simulations using the coarse-grained stochastic processes and reconstruction of microscopic scales. Derived a posteriori error control allows us to design adaptive coarse-graining of the configuration space. We shall briefly discuss how the methods of statistical mechanics (e.g., cluster expansions) lead to improved schemes with optimized interaction kernels. On specific examples of lattice as well as off-lattice dynamics (simulations of spin systems or polymers) we demonstrate that computational implementation of constructed hierarchical algorithms leads to significant speed up of simulations. Results from joint work with Markos Katsoulakis, Univ. of Massachusetts, Amherst and Vagelis Harmandaris, Max-Planck Institute for Polymers will be presented.

A Path-integral Formulation of DNA Looping Probabilities

John H. Maddocks¹, Rob Manning², Ludovica Cotta-Ramusino³

¹ **Faculté des Sciences de Base, École Polytechnique Fédérale de Lausanne, Lausanne, Switzerland (E-mail: john.maddocks@epfl.ch)**

² **Mathematics Department, Haverford College, Haverford, PA, USA; (E-mail: rmanning@haverford.edu)**

³ **Institute for Mathematics and its Applications, University of Minnesota, Minnesota, USA (E-mail: cottaram@ima.umn.edu)**

ABSTRACT

DNA looping is a biologically important phenomenon in which the probability of loop formation depends on the sequence of the fragment in question. I will show how such looping probabilities can be modelled using a semi-classical path integral formalism to evaluate approximations to the stationary probability density function for the location and orientation of one end of a continuum elastic rod, or polymer. The expression obtained involves the energy of a solution to the associated Euler-Lagrange equations arising from elasticity plus a fluctuation correction in terms of a volume of a basis of solutions to the associated Jacobi equations.

Mean Field Approximation of Transfer Operators in High-dimensional Conformation Dynamics

Gero Friesecke¹, Oliver Junge²

Center of Mathematics, TU Munich, Germany

¹gf@ma.tum.de; ²junge@ma.tum.de

ABSTRACT

Conformation transitions reflect the global spatial/temporal behaviour of the system, and in particular occur at much slower timescales compared to the elementary frequencies of the system, and are therefore difficult territory for trajectory based methods. Since the 1990s an alternative approach based on transfer operators acting on densities on phase space has been developed, notably by Deuffhard, Schuette and coworkers. In the latter approach, the number of computational degrees of freedom of a direct discretization scales exponentially in the number of atoms. To overcome this problem we have developed a mean field method for computing transfer operators, whose relationship to the exact transfer operator is reminiscent of that of Hartree-Fock theory to the many-particle Schroedinger equation in quantum chemistry. Applications to biomolecules will be presented.

Some Recent Progress in Elliptic Homogenization

Xavier Blanc^{1,3}, Claude Le Bris^{2,3}, Pierre-Louis Lions^{4,5}

¹Laboratoire J.-L. Lions, Université Pierre et Marie Curie, Boite courrier 187, 75252 Paris Cedex 05, France (E-mail: blanc@ann.jussieu.fr)

²CERMICS, Ecole Nationale des Ponts et Chaussées, 6 et 8 avenue Blaise Pascal, 77455 Marne-la-Vallée Cedex 2, France (E-mail: lebris@cermics.enpc.fr)

³INRIA Rocquencourt, MICMAC team-project, Domaine de Voluceau, BP 105, 78153 Le Chesnay Cedex, France

⁴Collège de France, 11, place Marcelin Berthelot, 75231 Paris Cedex 05, France

⁵CEREMADE, Université Paris Dauphine, place du Maréchal de Lattre de Tassigny, 75775 Paris Cedex 16, France (E-mail: lions@ceremade.dauphine.fr)

ABSTRACT

We will present a series of recent works related to elliptic homogenization: on the theoretical front, some variants of stochastic homogenization([1,2]), and on the numerical front, some approaches for improving the accuracy of corrector computations ([3], based on ideas previously developed in another context in [4,5]).

- [1] X. Blanc, C. Le Bris, P-L. Lions, Stochastic homogenization and random lattices, Journal de Mathématiques Pures et Appliquées, 88, pp 34-63, 2007
- [2] X. Blanc, C. Le Bris, P-L. Lions, Une variante de la théorie de l'homogénéisation stochastique des opérateurs elliptiques, Note aux Comptes Rendus de l'Académie des Sciences, t.~343, Série 1, p 711-724, 2006.
- [3] X. Blanc, C. Le Bris, in preparation.
- [4] E. Cancès, F. Castella, Ph. Chartier, E. Faou, C. Le Bris, F. Legoll, G. Turinici, High-order averaging schemes with error bounds for thermodynamical properties calculations by MD simulations, J. Chemical Physics, Volume 121, Number 21, 2004, pp~10346-10355
- [5] E. Cancès, F. Castella, Ph. Chartier, E. Faou, C. Le Bris, F. Legoll, G. Turinici, Long-time averaging for integrable hamiltonian dynamics, Numerische Mathematik, vol.135, Iss.2, 2005, pp211-232

Micro-macro FENE Models for Polymeric Materials and their Closure Approximations

Qiang Du

**Dept of Mathematics and Materials Science and Engineering,
Penn State University, University Park, PA 16802
(E-mail: qdu@math.psu.edu)
<http://www.math.psu.edu/qdu>**

ABSTRACT

We present some systematic moment closure methods for the multiscale micro-macro FENE models of polymeric materials, and demonstrate the good agreement of the new closure models with the fully coupled model in various cases that include the simple shear and extensional flows. This talk is based on the joint works with P. Yu (currently Goldman Sachs), C. Liu and Y. Hyon of Penn State University and J. Carrillo of Barcelona.

- [1] Q. Du, C. Liu and P. Yu, “FENE Dumbbell Model and Its Several Linear and Nonlinear Closure Approximations”, SIAM Multiscale Modelling and Simulations, 4, pp. 709-731, (2005)
- [2] Q. Du, C. Liu and P. Yu, From Micro to Macro Dynamics via a New Closure Approximation to the FENE Model of Polymeric Fluids,” SIAM Multiscale Modelling and Simulations, 3, pp. 895-917, (2005).
- [3] Y. Hyon, Q. Du and C. Liu, “An Enhanced Macroscopic Closure Approximation to the Micro-Macro FENE Models for Polymeric Materials”, SIAM Multiscale Modelling and Simulations, in press, (2008)
- [4] Y. Hyon, J. Carrillo, Q. Du and C. Liu, A Maximum Entropy Principle Based Closure Method for Macro-Micro Models of Polymeric Materials, Kinetic and Related Models, 1, pp.171-184, (2008)

Homogenization with Nonseparated Scales

Leonid Berlyand

Department of Mathematics, Pennsylvania State University, University Park, PA, USA
(E-mail : berlyand@math.psu.edu)

ABSTRACT

This is a joint work with H. Owhadi (Caltech). We discuss a novel mathematical approach that allows to construct discrete finite dimensional approximations with a controlled error estimate in continuum PDE models with non-separated scales. This approach is based on approximation of gradients of H^2 functions in L^2 norm by a linear combination of M divergence free vector fields from $(L^2(\Omega))^n$ with coefficients that are piecewise linear on a partition of the domain $\Omega \subset R^n$ of a given resolution h with an error of the order h . Here M is any integer greater than n . We apply this approach to upscaling of elasticity problems and, in particular, derive a generalized Cauchy-Born rule for non-monoatomic solids.

Toward Multiscale Modelling and Simulation of Fuel Cells

Ismaila Dabo^{1,2}, Eric Cancès^{1,2}, Yanli Li¹ and Nicola Marzari²

¹**Cermics, Ecole des Ponts, Université Paris Est, and INRIA Rocquencourt, Micmac Project, 6 & 8 avenue Blaise Pascal, Cité Descartes, 77455 Marne-la-Vallée, France,**

²**Department of Materials Science and Engineering, Massachusetts Institute of Technology, Cambridge, MA, USA.**

ABSTRACT

Understanding the electrical response of electrochemical convertors, such as fuel cells or batteries, involves elucidating the effect of the macroscopic voltage on the microscopic charge distribution at the electrode-electrolyte interface.

I will present a quantum/classical model which couples a quantum molecular description of the electrode-electrolyte interface with a polarizable-continuum representation of the long-range effects of the ionic solvent. I will mainly focus on the mathematical and numerical aspects. In the last part of my talk, I will present some numerical simulations which demonstrate the efficiency of this approach.

The authors acknowledge support from the MURI grant DAAD 19-03-1-0169, from the INRIA postdoctoral fellowship, and from the ANR CIS Sire grant.

Sub-linear Scaling Algorithms for the Study of the Electronic Structure of Materials

Carlos J. Garcia-Cervera¹, Jianfeng Lu², and Weinan E³

¹ **Mathematics Department, University of California, Santa Barbara, CA 93106,
(E-mail: cgarcia@math.ucsb.edu)**

² **Program in Applied and Computational Mathematics, Princeton University, Fine Hall,
Washington Road, NJ 08544 (E-mail: jianfeng@math.princeton.edu)**

³ **Mathematics Department and Program in Applied and Computational Mathematics,
Princeton University, Fine Hall, Washington Road, NJ 08544,
(E-mail: weinan@princeton.edu)**

ABSTRACT

We discuss a class of sub-linear scaling algorithms for the study of the electronic structure of materials, based on a real-space formulation of the Kohn-Sham density functional theory in terms of non-orthogonal, localized orbitals. We divide these localized orbitals into two sets: One set associated with the atoms in the region where the deformation of the material is smooth (smooth region), and other set associated with the atoms around the defects (non-smooth region). The orbitals associated with atoms in the smooth region can be approximated accurately using asymptotic analysis. The results from the smooth region can then be used to find the orbitals in the non-smooth region.

[1] C.J. Garcia-Cervera, J. Lu, and W. E, “A sub-linear scaling algorithm for computing the electronic structure of materials”, *Communications in Mathematical Sciences*, **5**, 999 (2007).

The work of E and Lu is supported in part by ONR grant N00014-01-1-0674, DOE grant DOE DE-FG02-03ER25587, NSF grants DMS-0407866 and DMR-0611562. The work of Garcia-Cervera is partially supported by and NSF CAREER award, DMS-0645766.

BOSSANOVA: A bond order dissection approach for efficient electronic structure calculations

Michael Griebel, Jan Hamaekers, Frederik Heber
 Institute for Numerical Simulation, Wegelerstrasse 6,
 53115 Bonn, Germany, heber@ins.uni-bonn.de

Abstract

We propose a general coupling method in the context of additivity models, see references in [1], and of general fragmentation schemes such as [2, 3] for the efficient numerical treatment of the electronic structure problem of molecular systems. We discuss the new method which results in linear scaling complexity and demonstrate its qualities for a wide range of organic molecules.

1 Method

The coupling of the micro- and the mesoscale of molecular systems and their chemical reactions is currently a field of intensive research. Here, the ultimate goal would be a seamless coupling of quantum mechanical computations where needed and classical molecular mechanics simulations where sufficient. To this end, we consider the time-independent electronic Schrödinger equation in the Born-Oppenheimer approximation,

$$\mathcal{H}_e^{\mathbf{R}(t)}(\mathbf{r})\phi_{(0)}^{\mathbf{R}(t)}(\mathbf{r}) = E_0(\mathbf{R}(t))\phi_{(0)}^{\mathbf{R}(t)}(\mathbf{r}), \quad (1)$$

where $\mathbf{R}(t)$ represents the time-dependent $3M$ nuclei coordinates, r the $3N$ electronic degrees of freedom and ϕ_0 designates the electronic ground state wave function with energy E_0 of the Hamiltonian \mathcal{H}_e . We then define a total ground state energy function $E^{(M)} : (\mathbb{N} \times \mathbb{R}^3)^M \rightarrow \mathbb{R}$.

$$E^{(M)}(\tilde{\mathbf{R}}_I) := \min_{\left| \phi_{(0)}^{(\tilde{\mathbf{R}}_I)} \right| = 1} \int \phi_{(0)}^{(\tilde{\mathbf{R}}_I)*}(\mathbf{r}) \mathcal{H}_e \phi_{(0)}^{(\tilde{\mathbf{R}}_I)}(\mathbf{r}) d\mathbf{r}, \quad (2)$$

where $\phi_{(0)}$ denotes the ground state electronic wave function, $\tilde{R}_i := (Z_i, R_i(t))$ denotes the set of variables $\{\tilde{R}_i\}_{i \in U}$ with the index set $I = \{1, \dots, M\}$ of the nuclei and $R_i(t)$ and Z_i denotes the nuclei coordinates and the atomic number of each nuclei, respectively.

Now, we decompose the energy function $E^{(M)}$ analogously to the ANOVA approach, for further details of the ANOVA decomposition see [4] and the references given therein. To this end, we expand the $3M$ -dimensional function $E^{(M)}$ in a multivariate telescopic sum, involving a splitting into contributions which depend on the positions of single nuclei and associated charges, of pairs of nuclei and associated charges, of triples of nuclei and charges, and so on, i. e.,

$$\begin{aligned} E^{(M)}(\tilde{R}_1, \dots, \tilde{R}_M) &:= \sum_{U \subseteq I} F_U(\tilde{R}_U) \\ &= F_0 + \sum_{i_1}^M F_{i_1}(\tilde{R}_{i_1}) + \sum_{i_1 < i_2}^M F_{i_1, i_2}(\tilde{R}_{i_1}, \tilde{R}_{i_2}) + \dots + F_{i_1, \dots, i_M}(\tilde{R}_{i_1}, \dots, \tilde{R}_{i_M}). \end{aligned} \quad (3)$$

Here, each term F_{i_1, \dots, i_k} is defined as follows:

$$\begin{aligned} F_{i_1}(\tilde{R}_{i_1}) &= E_{i_1}(\tilde{R}_{i_1}) - F_0, \\ F_{i_1, i_2}(\tilde{R}_{i_1}, \tilde{R}_{i_2}) &= E_{i_1, i_2}(\tilde{R}_{i_1}, \tilde{R}_{i_2}) - F_{i_1}(\tilde{R}_{i_1}) - F_{i_2}(\tilde{R}_{i_2}) - F_0, \\ &\dots \quad \dots, \end{aligned} \quad (4)$$

where the constant function F_0 is set equal to zero since it corresponds to the energy of an empty molecular system. The total electronic ground state energy $E_U(\tilde{R}_U)$ of a molecular subsystem, described by a set of indices $U \subseteq I$, is then defined in an analogous way to (2).

The energy functions F_{i_1, \dots, i_k} may be considered as many-body interaction contributions, as in [5]. This leads us to the following assumption: There is a certain decay with the order $|U| = k$ of the contributions in the ANOVA expansion. This is also strongly supported by the success of conventional two-, three-, four- and many-body potential functions used in classical molecular mechanics. Hence, we truncate the series expansion (3) at a defined order k by setting

$$E^{(M)}(\tilde{R}_1, \dots, \tilde{R}_M) \approx \sum_{U \subseteq I} \gamma_U F_U(\tilde{R}_U) \quad \text{with } \gamma_U = \begin{cases} 0 & |U| > k, \\ 1 & |U| \leq k. \end{cases} \quad (5)$$

Furthermore, we interpret a molecular system with M nuclei as a hydrogen-suppressed graph $G_I = (V_I, E_I)$ with vertex set $V_I = \{v_i\}_{i \in I}$ and edge set $E_I = \{e_{ij}\}_{i, j \in I}$ of all

bonds, where each edge of E_I corresponds to a bond between vertices $v_i, v_j \in V_I$ in the system. Furthermore, we define the distance matrix, see [6],

$$D_{ij} = \begin{cases} \min(l(p_{ij})) & \exists e_{ij} \in E_I, \\ +\infty & e_{ij} \notin E_I, \end{cases} \quad (6)$$

where $\min(l(p_{ij}))$ is the shortest path for all vertices $v_i, v_j \in V_I$. Now, consider for example the term $F_{i_1, i_2}(\tilde{R}_{i_1}, \tilde{R}_{i_2})$ in (5), which represents a two-body interaction. If we disassociate the two atoms $\tilde{R}_{i_1}, \tilde{R}_{i_2}$, i. e. if we take the limit $|\tilde{R}_{i_1} - \tilde{R}_{i_2}| \rightarrow \infty$, the energy term will be just the sum of the single particle energies: $E_{i_1, i_2}(\tilde{R}_{i_1}, \tilde{R}_{i_2}) \rightarrow E_{i_1}(\tilde{R}_{i_1}) + E_{i_2}(\tilde{R}_{i_2})$. Hence, $\lim_{|\tilde{R}_{i_1} - \tilde{R}_{i_2}| \rightarrow \infty} F_{i_1, i_2}(\tilde{R}_{i_1}, \tilde{R}_{i_2}) = 0$. Analogous observations hold for higher order terms. Consequently, we also drop terms in (5) by further setting

$$\gamma_U = \begin{cases} 0 & \max\{D_{ij} | \forall i, j \in U \text{ with } i \neq j\} > k, \\ 1 & \text{else,} \end{cases} \quad (7)$$

for details see [7]. Then, according to their non-zero values γ_U we identify the resulting fragments U . Note that for all F_U with $\gamma_U \neq 0$ according to (4) we only need to know terms E_U and $F_{U'}$ with $U' \subseteq U$ and $\gamma_{U'} \neq 0$. We solve each eigenvalue problem of the related local Hamiltonian of the Schrödinger equation by an approximate solver such as Hartree-Fock or DFT that yields the energies E_U . Finally, we compute first all necessary terms F_U by the recursion relation (4) and then we form the truncated sum in (5), which gives a good approximation of $E^{(M)}$.

This scheme, coined Bond Order diSSection ANOVA, results in a linear scaling complexity. Accordingly, the overall evaluation cost of the eigenvalue problems, as the number of involved terms in the series expansion, depends only linearly on the number of nuclei M . Thus, this scheme is attractive for huge systems up to thousands and ten thousands atoms: It is trivial to parallelize and scales directly with the number of processors. Furthermore, it requires only very moderate resources per local electronic problem and is thus ideal for cluster computing.

This also has an important impact on QM/MM molecular dynamics simulations and specifically on multi-scale coupling schemes, where for thousands of small time steps a huge number of fragments will have to be calculated. There, a passive environment is modelled via empirical potentials and only the active region - called the reaction site - is treated quantum mechanically.

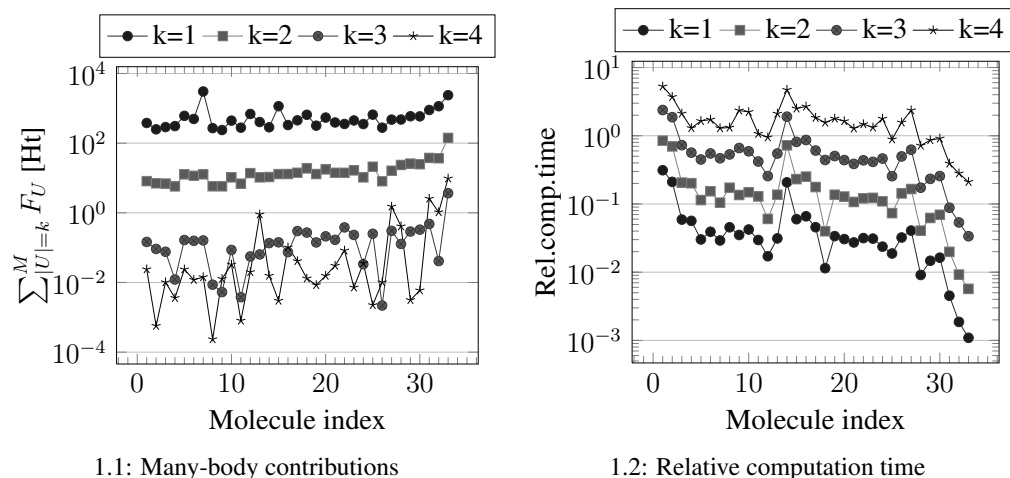


Figure 1: Magnitude of summed contributions $\sum_{|U|=k}^M F_U$ for each truncation order k in Hartree and relative computation time per order k .

2 Numerical Results

We applied the method to a wide range of organic molecules, the specifics are given in table 1, where we have sorted the molecular configurations first by the number of rings and second by the number of atoms in ascending order. In the implementation of our BOSSANOVA method, we employed for each of the fragments E_U standard closed shell Hartree-Fock calculations and the STO-3G basis set. We used the "Massively Parallel Quantum Chemistry" program [8].

In fig. 1.1 we give the summed contributions $\sum_{|U|=k}^M F_U$ of each order k in Hartree, in fig. 1.2 the computation time up to the specific order k in relation to the time for a calculation of the total system. We clearly see a fast decay of the summed contributions with rising order k . This indicates good convergence. Correspondingly, a relative computation time less than 1 indicates faster overall computation. Noticeably, our scheme performs very well and outruns full calculations on molecules, whose graphs have a tree-like structure, up to order $k = 3$ already for small systems $M < 10$. Molecules with many interconnected rings, as found for higher index numbers in fig. 1.1 and 1.2, have to be treated with values of k larger than the size of the rings, as these still give a significant many-body contribution.

Funding was granted under the priority program SPP1165 of the Deutsche Forschungsgemeinschaft (DFG).

Table 1: Suite of test molecules and their indices.

INDEX	MOLECULE	INDEX	MOLECULE	INDEX	MOLECULE
1	oxalic acid	12	glucose	23	acetanilide
2	acrylamide	13	proline	24	2-methylcyclohexanone
3	(N,N)-dimethylacetamide	14	(1,3,5)-triazine	25	aspirin
4	(1,2)-dimethoxyethane	15	(1,4)-dichlorobenzene	26	cycloheptane
5	tartaric acid	16	benzonitrile	27	adenine
6	asparagine	17	melamine	28	biphenylene
7	dimethyl bromomalonate	18	gallic acid	29	benzophenone
8	putrescine	19	(1,2)-dimethylbenzene	30	benzidine
9	neohexane	20	mandelic acid	31	indigo
10	isoleucine	21	m-methylanisole	32	cholesterol
11	heptan	22	2-phenylpropene	33	buckyball

References

- [1] M. Y. Hayes, B. Li, and H. Rabitz. Estimation of molecular properties by high-dimensional model representation. *Journal of Physical Chemistry*, 110:264–272, 2006.
- [2] N. Gresh, P. Claverie, and A. Pullman. Theoretical studies of molecular conformation. Derivation of an additive procedure for the computation of intramolecular interaction energies. Comparison with ab-initio SCF computations. *Theoretica Chimica Acta*, 66:1–20, 1984.
- [3] M. A. Collins and V. A. Deev. Accuracy and efficiency of electronic energies from systematic molecular fragmentation. *Journal of Chemical Physics*, 125:104104–1 – 104104–15, 2006.
- [4] M. Griebel. Sparse grids and related approximation schemes for higher dimensional problems. In L. Pardo, A. Pinkus, E. Suli, and M.J. Todd, editors, *Foundations of Computational Mathematics (FoCM05)*, Santander, pages 106–161. Cambridge University Press, 2006.
- [5] D. Marx and J. Hutter. Ab initio molecular dynamics: Theory and implementation. In *Modern Methods and Algorithms of Quantum Chemistry*, volume 1 of *NIC Series*, pages 301–440. Forschungszentrum Juelich, Deutschland, 2000.
- [6] R. B. King, editor. *Chemical Applications of Topology and Graph Theory*. Elsevier, 1983.
- [7] M. Griebel, J. Hamaekers, and F. Heber. BOSSANOVA: A bond order dissection approach for efficient electronic structure calculations. INS Preprint 0704, Institut für Numerische Simulation, Universität Bonn, January 2008.
- [8] C. Janssen, E. Seidl, and M. Colvin. Object-oriented implementation of parallel ab initio programs. In *ACS Symposium Series, Parallel Computing in Computational Chemistry*, volume 592, 1995.

Adaptive Control of Modeling Error for Multiscale Simulations

J. Tinsley Oden, Serge Prudhomme, Paul T. Bauman, and Ludovic Chamoin

**Institute for Computational Engineering and Sciences, The University of Texas at Austin,
1 University Station C0200, Austin, TX 78712, U.S.A.**

**(E-mails: oden@ices.utexas.edu, serge@ices.utexas.edu, pbauman@ices.utexas.edu,
ludo@ices.utexas.edu)**

ABSTRACT

In this talk, we describe a general approach for estimating and controlling modeling error, defined here as the difference between values of quantities of interest theoretically attainable by a fine-scale base model and those values supplied by a sequence of coarser-scale surrogate models. This approach provides the basis for goal-oriented error estimation and adaptation for multi-scale problems [1,2,3,4] and we give examples of modeling error estimation and adaptive modeling in which the sequences of surrogate models are obtained using atomic-to-continuum coupling methods. To demonstrate the effectiveness of this framework, we consider a class of applications in molecular statics of large polymer structures encountered in manufacturing nano-scale semiconductor devices [5]. We also describe more recent work on extending these concepts to stochastic systems and present new Bayesian-based approaches to calibration, validation, and uncertainty quantification for multiscale modeling.

- [1] J.T. Oden and S. Prudhomme, “Estimation of Modeling Error in Computational Mechanics”, *Journal of Computational Physics*, **182**, 496 (2002).
- [2] S. Prudhomme, P.T. Bauman, and J.T. Oden, “Error Control for Molecular Statics Problems”, *International Journal for Multiscale Computations in Engineering*, **4**, 647 (2006).
- [3] J.T. Oden, S. Prudhomme, A. Romkes, and P.T. Bauman, “Multiscale Modeling of Physical Phenomena: Adaptive Control of Models”, *SIAM Journal of Scientific Computing*, **28**, 2359 (2006).
- [4] S. Prudhomme, L. Chamoin, H. Ben Dhia, and P.T. Bauman, “An Adaptive Strategy for the Control of Modeling Error in Two-dimensional Atomic-to-Continuum Coupling Simulations”, *Computer Methods in Applied Mechanics and Engineering*, (Submitted).
- [5] P.T. Bauman, J.T. Oden, and S. Prudhomme, “Adaptive Multiscale Modeling of Polymeric Materials with Arlequin Coupling and Goals Algorithms”, *Computer Methods in Applied Mechanics and Engineering*, (Submitted).

Support of this work by DOE under contract DE-FG02-05ER25701 is gratefully acknowledged. Collaborative discussions on aspects of the Arlequin method with H. Ben Dhia of the Laboratoire de Mécanique des Sols, Structures et Matériaux (LMSSMAT) at Ecole Centrale de Paris, France, are greatly appreciated.

A New Frontier of Kinetic Theory Applications in Solid Mechanics— The Discrete-Continuum Connection in Dislocation Dynamics

Anter El-Azab

**School of Computational Science (and Materials Science Program), Florida State
University, Tallahassee, FL 32306; E-mail: anter@scs.fsu.edu**

ABSTRACT

The problem of developing continuum models of dislocation dynamics in metallic crystals is addressed in this work. This multiscale problem is important in developing a physical theory of crystal plasticity from first principles: the statistics, dynamics and interactions of dislocations. A formalism of the problem is developed here by adopting the concepts of classical kinetic theory. In particular, we derive a hierarchical set of kinetic equations governing the space-time evolution of the dislocation density in the crystal, which is similar to Klimontovich's development of the kinetic theory of plasma [1]. We further analyze the coupling of the dislocation density evolution with the long-range dislocation interactions and with the changes in the crystal geometry induced by plastic distortion. A proposal for a crystal plasticity theory based on this statistical mechanical framework will be given and compared with existing empirically-based theories.

[1] Yu. L. Klimontovich, *The Statistical Theory of Non-Equilibrium Processes in a Plasma*, MIT Press, Cambridge, MA, 1967.

The work is supported by the U.S. Department of Energy, Office of Basic Energy Sciences, Division of Materials Science and Engineering under contract number DE-FG02-08ER46494 at Florida State University.

Electronic Structure Calculations at Macroscopic Scales

Vikram Gavini

**Department of Mechanical Engineering, University of Michigan, Ann Arbor, MI 48109
(E-mail: vikramg@umich.edu)**

ABSTRACT

Electronic structure calculations (derived from first-principle, quantum-mechanical calculations), especially those using density-functional theory have provided many insights into various materials properties in the recent decade. However, the computational complexity associated with electronic structure calculations has restricted these investigations to periodic geometries with cell-sizes consisting of few atoms (200 atoms). But, material properties are influenced by defects in small concentrations (parts per million). A complete description of such defects must include both the electronic structure of the core at the fine (sub-nanometer) scale and also elastic and electrostatic interactions at the coarse (micrometer and beyond) scale. This in turn requires electronic structure calculations at macroscopic scales, involving millions of atoms, well beyond the current capability.

This talk presents the development of a seamless multi-scale scheme, quasi-continuum orbital-free density-functional theory (QC-OFDFT) to perform electronic structure calculations at macroscopic scales. This multi-scale scheme has enabled for the first time a calculation of the electronic structure of multi-million atom systems using orbital-free density-functional theory, thus, paving the way to an accurate electronic structure study of defects in materials. The key ideas in the development of QC-OFDFT are (i) a real-space variational formulation of orbital-free density-functional-theory, (ii) a nested finite-element discretization of the formulation, and (iii) a systematic means of adaptive coarse-graining retaining full resolution where necessary, and coarsening elsewhere with no patches, assumptions or structure. Rigorous proofs of convergence of the finite-element approximation using the variational notion of Gamma-convergence will be presented. The accuracy of QC-OFDFT scheme and the physical insights it offers into the behavior of defects in materials are highlighted by the study of vacancies in aluminum.

This work is done in joint collaboration with Prof. Michael Ortiz (Caltech), Prof. Kaushik Bhattacharya (Caltech), and Dr. Jaroslaw Knap (ARL).

A Numerical Bridge Between Quantum and Molecular Dynamics based on the Ehrenfest Dynamics

D. Aubry, A.-L. Hamon

**Ecole Centrale Paris, MSSMat, 92290 Chatenay-Malabry, France
(E-mails: denis.aubry@ecp.fr, ann-lenaig.hamon@ecp.fr)**

ABSTRACT

The classical approach [1] in molecular dynamics is to apply Newton's laws to each nucleus submitted to forces deriving from potentials themselves built and fitted from computational quantum mechanics. Obviously the displacement of the nuclei modifies the potential but this effect is not always taken into account or only through an outer loop. But in several cases the inter-nuclei coupling is not local because the electronic density may be distributed far away and full coupling has to be considered.

We propose here to follow two ideas to circumvent these shortcomings. The first one is to apply the Ehrenfest dynamics [2] for the transition from quantum to molecular dynamics because it is more basically linked to the probability signification of the wave function and incorporates its spatial distribution. For instance for a 2-body problem it provides a relation of the following qualitative type:

$$\langle x_n \rangle'' = \frac{-1}{m_n} \langle \nabla_n V |\psi(x_n, x_e)|^2 \rangle$$

which shows that the Newton law is actually a weighted wave average of the potential gradient ∇V by the wave function $\psi(x_n, x_e)$ which depends both on electron and atomic positions.

The second idea is to revisit the decoupling between quantum and molecular dynamics [3]. Actually because of the Born approximation the nuclei are assumed to be fixed during the *ab initio* computations although the position of the atoms has to be iteratively modified in order to arrive at a true ground state energy. The algorithm that we propose here is to reach directly this state by an explicit coupling between quantum and molecular computations as is often used e.g. in dynamic relaxation approaches in nonlinear structural dynamics.

REFERENCES

- [1] F.A. Bornemann, C. Schoutte , “On the singular limit of the quantum-classical molecular dynamics model”, *SIAM J. Appl. Math.* , Vol. **59**, pp. 1208–1224, (1999).
- [2] S. Gasirowicz, *Quantum physics*, Wiley, 1996.
- [3] J.M. Thijssen, *Computational physics*, Cambridge University Press, 1999.

On a Stochastic Approach for Atomic-to-Continuum Coupling Methods

Ludovic Chamoin, Serge Prudhomme, J. Tinsley Oden, and Paul T. Bauman

Institute for Computational Engineering and Sciences, The University of Texas at Austin, 1
University Station C0200, Austin, TX 78712, U.S.A
(E-mails: ludo@ices.utexas.edu, serge@ices.utexas.edu, oden@ices.utexas.edu,
pbauman@ices.utexas.edu)

ABSTRACT

In this work, we develop a coupling method to perform multi-scale Monte-Carlo simulations of material structures described at the atomic scale and subjected to random phenomena. The new method results in a dramatic reduction of the number of degrees of freedom that would be required if one wanted to perform Monte-Carlo simulations of the fully atomic structure. The focus here is on the construction of an equivalent stochastic continuum model and on the coupling of this model with a discrete particle model through a stochastic version of the Arlequin Method [1,2]. Concepts from the Stochastic Finite Element Method, such as the Karhunen-Loeve expansion and Polynomial Chaos, as well as Stochastic Collocation, are extended here to multi-scale problems so that Monte-Carlo simulations are performed only with respect to the sub-regions of interest. Preliminary results are given for 1D and 2D structures with harmonic interaction potentials [3,4].

- [1] H. Ben Dhia and G. Rateau, “The Arlequin Method as a Flexible Engineering Design Tool”, *International Journal for Numerical Methods in Engineering*, **62**, 1442 (2005).
- [2] P.T. Bauman, H. Ben Dhia, N. Elkhodja, J.T. Oden, and S. Prudhomme, “On the Application of the Arlequin Method to the Coupling of Particle and Continuum Models”, *Computational Mechanics*, **42**, 511 (2008).
- [3] L. Chamoin, J.T. Oden, and S. Prudhomme, “A Stochastic Coupling Method for Atomic-to-Continuum Monte-Carlo Simulations”, *Computer Methods in Applied Mechanics and Engineering*, (In Press, Available online April 2008).
- [4] L. Chamoin, J.T. Oden, and S. Prudhomme, “Engineering Problems in Materials Science Coupling Atomic and Continuum Models with Random Data - Formulation and Solution using a Stochastic Collocation Method”, (In preparation).

Support of this work by DOE under contract DE-FG02-05ER25701 is gratefully acknowledged. Collaborative discussions on aspects of the Arlequin method with H. Ben Dhia of the Laboratoire de Mécanique des Sols, Structures et Matériaux (LMSSMAT) at Ecole Centrale de Paris, France, are greatly appreciated.

Mathematical Validation and Algorithms for the Quasicontinuum Method

Mitchell Luskin, Marcel Arndt, Matthew Dobson

School of Mathematics, University of Minnesota
206 Church St. SE, Minneapolis, Minnesota 55455
(E-mail: luskin@umn.edu)

ABSTRACT

The development of predictive and efficient atomistic-to-continuum computational methods requires both an analysis of the error and efficiency of its many components (coupling error, model and mesh adaptivity, solution methods) as well as its integration into an efficient method capable of solving problems of technological interest. Mathematical challenges are presented by the complex energy landscape of materials with defects and microstructure, where the classical numerical analysis techniques developed for convex energy landscapes and elliptic partial differential equations is inadequate.

For crystalline materials, there are typically a few small regions with highly non-uniform structure caused by defects in the material which are surrounded by large regions where the local environment of the atoms varies slowly. The idea of the Quasicontinuum Method is to achieve accuracy similar to a fully atomistic simulation while reducing the computational complexity in regions where the strain gradient is small. It does so by selecting representative atoms as nodes for piecewise linear interpolation and by further approximating the nonlocal atomistic energy by a local strain energy density. Since the position of material defects is typically not known *a priori*, we have developed adaptive algorithms to determine where the accuracy of atomistic modeling is needed and how to coarsen the mesh in the continuum region.

There are many choices available for the interaction among the representative atoms, especially between those in the atomistic and continuum regions, which has led to the development of a variety of quasicontinuum approximations. We will present criteria for determining a good choice of quasicontinuum approximation for a given problem that considers trade-offs between accuracy and algorithmic efficiency. Our criteria are based on an analysis of the effect of the coupling error on the goal of the computation, on the integration of the quasicontinuum approximation with model and mesh adaptivity, and on the development of efficient iterative solution methods.

See <http://www.math.umn.edu/~luskin/cv/papers.html> for references.

Comparing the Accuracy and Efficiency of Multiscale Methods

Ronald E. Miller¹, Ellad B. Tadmor² and Mitchell Luskin³

¹**Department of Mechanical and Aerospace Engineering, Carleton University, 1125 Colonel By Drive, Ottawa, ON K1S 5B6, Canada (E-mail: rmiller@mae.carleton.ca)**

²**Aerospace Engineering and Mechanics, University of Minnesota, 110 Union St SE, Minneapolis, MN 55455, USA**

³**School of Mathematics, University of Minnesota, 206 Church St. SE, Minneapolis, MN 55455 USA**

ABSTRACT

In recent years there has been a multitude of new methods developed to couple an atomistic model to a continuum-based approximation (such as finite elements). The goal of these methods is to be able to reproduce the results of a fully atomistic simulation at a reduced computational cost. Naturally each of these methods has an inherent accuracy and efficiency, however it is difficult to compare these attributes between methods for two reasons. First, it is necessary to spell out what is a suitably rigorous yet sufficiently simple and controllable test problem to study as a benchmark for these methods. Second, it is necessary to implement all these methods within a unified overall framework. This eliminates any differences between elements that are common across methods (such as, for instance, routines to compute atomic forces or solver algorithms), and thus permits a fair comparison.

In this presentation, we make a case for what should be considered an appropriate benchmark problem; one that is sufficiently simple so as to be quick to simulate and straightforward to analyze, but not so simple as to unwittingly hide differences between methods. For example, models of 1D chains of atoms, or those using simple near-neighbor pair potentials are often not a sufficiently rigorous test. At the same time, the problem should test the model outside a simple linear or even elliptical regime. To this end, we have chosen to test all of the implemented methods on a problem involving the structure and motion of a dislocation dipole in fcc aluminum. The problem is 2D (actually 3D with minimal periodicity in the third direction) and uses a reasonably complex description of atomic bonding (the Embedded Atom Method potentials of Ercolessi and Adams).

Finally we have implemented 11 of the multiscale methods from the literature and compared their accuracy and efficiency on the dislocation dipole benchmark test. This allows direct, quantitative comparison between the accuracy and efficiency of these methods.

1D Atomistic-to-Continuum Coupling via Optimization

J. P. Reese, Max Gunzburger

Department of Scientific Computing, Florida State University, Dirac Science Library,
Tallahassee, FL 32306-4120; jreese@scs.fsu.edu, gunzburg@scs.fsu.edu

ABSTRACT

We consider an optimization-based atomistic-to-continuum coupling strategy where the atomistic and continuum displacements and stresses are constrained to agree over some overlap region where both models hold. A simple 1D example illustrates the optimization scheme.

1. Introduction

Multiscale simulations leverage the accuracy of microscale simulations in regions where the physics are rapidly changing while taking advantage of the efficiency of macroscale simulations in the remainder of the domain. We are interested in the case where the computational domain Ω is divided into three disjoint regions: Ω_a , where the physics of the problem are governed only by first principles at the microscale; Ω_c where a macroscale model holds; and Ω_b which is some *bridge region* acting as an interface between the two models.

In the literature, agreement between the two models is achieved mainly through constraining the microscale dynamics based on macroscale information [1] or using Schwarz iteration to guarantee consistency between the models [2]. However, this paper describes an optimization-based coupling strategy which in [3, 4] was applied to two *macroscale* regions, each governed by a different partial differential equation (PDE). The difference in this paper is that optimization over the bridge region is used to couple a microscale atomistic model over $\Omega_a \cup \Omega_b$ with a macroscale continuum model over $\Omega_b \cup \Omega_c$.

2. Models

2.1 Atomistic

The division of Ω into the three subdomains is effected in the reference configuration, \mathbf{X} . We let \mathcal{N}_a be the set of indices of particles located in $\Omega_a / (\Omega_a \cap \Omega_b)$, and \mathcal{N}_b be the set of particle indices located in Ω_b . The reference position of particle α is denoted by \mathbf{X}_α , while its deformed position is given by \mathbf{x}_α . Thus $\mathbf{u}_\alpha = \mathbf{x}_\alpha - \mathbf{X}_\alpha$ is the displacement of the α particle.

The force on particle α is assumed local and due only to particles within the ball $\mathcal{B}_\alpha = \{\mathbf{x} \in \Omega : |\mathbf{x} - \mathbf{x}_\alpha| \leq \eta\}$ for some given $\eta \geq 0$. Let $\mathcal{N}_\alpha = \{\beta | \mathbf{x}_\beta \in \mathcal{B}_\alpha, \beta \neq \alpha\}$, i.e. \mathcal{N}_α is the set of indices

corresponding to the particles in \mathcal{B}_α , other than the α particle itself. Then, the force on the atomistic particle α due to all the other particles is given by

$$\sum_{\beta \in \mathcal{N}_\alpha} \mathbf{f}_{\alpha,\beta} = 0 \quad \text{for } \alpha \in \mathcal{N}_a \cup \mathcal{N}_b, \quad (1)$$

where $\mathbf{f}_{\alpha,\beta}$ denotes the force acting on particle α due to particle β .

We do not apply the atomistic model to particles in Ω_c ; however, some particles in $\bar{\Omega}_a \cup \bar{\Omega}_b$ depend upon force contributions from particles in Ω_c . When the atomistic displacement of a particle in Ω_c is required, we assume it is equivalent to the continuum displacement, $\mathbf{u}(\mathbf{X})$.

2.2 Continuum Model

The Cauchy stress tensor, $\boldsymbol{\sigma}(\mathbf{X})$, is used to determine the force over the continuum region. At any point \mathbf{X} in the continuum region, we have the force balance

$$\nabla \cdot \boldsymbol{\sigma} + \mathbf{b}_c = 0 \quad \text{for } \mathbf{X} \in \bar{\Omega}_c \cup \bar{\Omega}_b \quad (2)$$

where \mathbf{b}_c is an externally applied volumetric force. In §4., we assume $\mathbf{b}_c = 0$.

3. Optimization Scheme

Over Ω_b both models hold, so the atomistic and continuum displacements and stresses should agree in the bridge region. The displacement constraint is expressed as

$$\mathbf{u}_\alpha = \mathbf{u}(\mathbf{X}_\alpha) \quad \text{for all } \alpha \in \mathcal{N}_b. \quad (3)$$

The stress constraint,

$$\boldsymbol{\sigma}_a^\alpha = \boldsymbol{\sigma}(\mathbf{X}_\alpha) \quad \text{for all } \alpha \in \mathcal{N}_b \quad (4)$$

requires an averaged ‘‘atomistic stress’’, $\boldsymbol{\sigma}_a^\alpha$, based on the computed atomistic displacements. This expression is given by

$$\boldsymbol{\sigma}_a^\alpha = \frac{1}{2|\Delta_\alpha|} \sum_{j \neq i} d_{ij} (\mathbf{x}_i - \mathbf{x}_j) \otimes \mathbf{f}_{i,j} \quad (5)$$

where the summation runs over all pairs of particles in the domain Ω , and the averaging is performed over the representative volume element, Δ_α [5]. The weighting function, d_{ij} , is determined by the fraction of $|\mathbf{x}_i - \mathbf{x}_j|$ that overlaps Δ_α .

We separately solve the atomistic model in Ω_a and the continuum model in Ω_c by specifying the displacements for the two models along Ω_b in such a way that

$$\mathbf{u}(\mathbf{X}) = \mathbf{U}(\mathbf{X}) \quad \text{for } \mathbf{X} \in \Omega_b \quad \text{and} \quad \mathbf{u}_\alpha = \mathbf{U}(\mathbf{X}_\alpha) \quad \text{for } \mathbf{X}_\alpha \in \Omega_b \quad (6)$$

for some guess displacement $\mathbf{U}(\cdot)$. Arbitrary choices for $\mathbf{U}(\cdot)$ will not satisfy (4), so the optimal $\mathbf{U}(\cdot)$ is found by solving the optimization problem

$$\min_{\mathbf{U}} \|\sigma_a^\alpha - \sigma(\mathbf{X}_\alpha)\|, \quad (7)$$

where σ_a^α and $\sigma(\mathbf{X})$ are determined from solving Eqns. (1) and (2) separately using the boundary conditions in Eqn. (6).

4. Numerical Example

Region $\Omega = (0, 1)$ is divided into Ω_a , Ω_b , and Ω_c . Fig. 1 shows the scenario of interested in this section: $\Omega_a = (0, 0.6)$, $\Omega_b = (0.3, 0.6)$, and $\Omega_c = (0.3, 1)$. The atomistic grid spacing is $s = 0.005$ while the continuum grid spacing is $h = 0.1$. The Δ_t used here is 0.05.

To test the algorithm described in §3., we consider the nearest-neighbor atomistic force model

$$f_{\alpha,\beta} = 100 \sum_{\beta=\alpha\pm 1} \left(\frac{u_\alpha - u_\beta}{s} \right), \quad (8)$$

and a continuum stress model given by

$$\sigma(u) = 100 \frac{du}{dx}. \quad (9)$$

The exact displacement solution is linear from $u(0) = 0$ to $u(1) = 0.01$, which leads to a constant exact stress solution of one over the whole domain. The initial guess for the displacement is exactly zero, and Matlab's `fmincon` function is used to find the optimal solution with objective function and constraint tolerances of 10^{-6} .

The optimal linear displacement and stress are shown in Fig. 1. One can see that the displacement is well-approximated, and the atomistic and continuum stresses agree with the exact solution up to the 4th decimal place. The optimizer reached this solution after six iterations and 868 function calls. The objective function was reduced to 6.6441×10^{-11} , and the maximum constraint value was 7.903×10^{-8} .

5. Summary

We have illustrated a method for coupling atomistic and continuum simulations using optimization. While the numerical example showed only a simple one-dimension problem with nearest-neighbor atomistic interactions, this procedure can be extended to more complicated coupling problems.

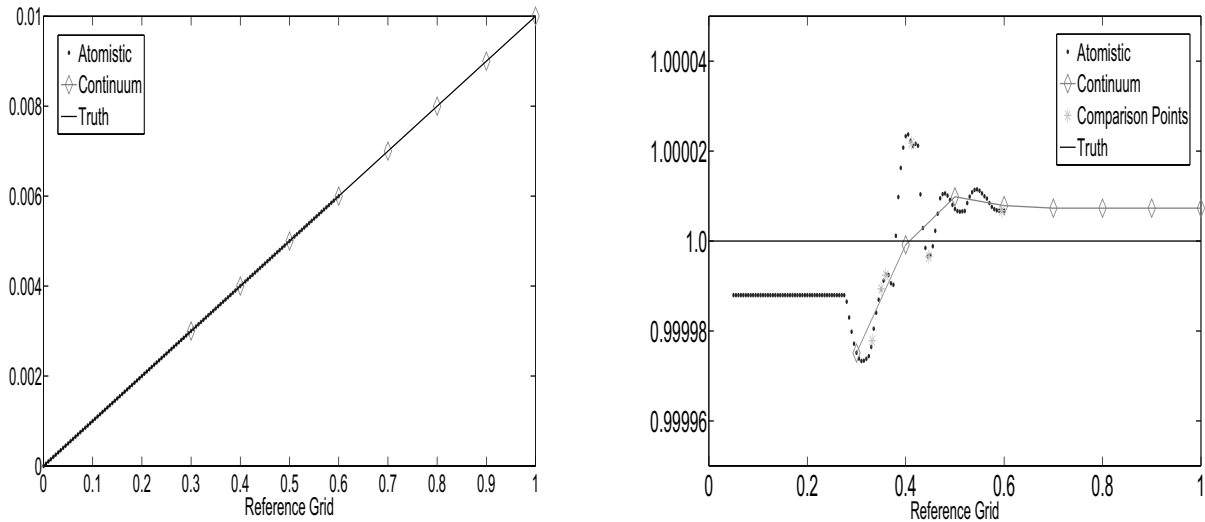


Figure 1: Nearest neighbor interactions, overlap at $[0.3, 0.6]$: displacement (left) and stress (right)

Acknowledgements

This work was supported by the Office of Science of the U.S. Department of Energy under grant number DE-FG02-05ER25698.

References

- [1] X. B. Nie, S. Y. Chen, W. N. E, and M. O. Robbins, “A Continuum and Molecular Dynamics Hybrid Method for Micro- and Nano-fluid Flow”, *Journal of Fluid Mechanics*, **500**, 55 (2004).
- [2] E. M. Kotsalis, J. H. Walther, and P. Koumoutsakos, “Control of Density Fluctuations in Atomistic-Continuum Simulations of Dense Liquids”, *Physical Review E*, **76**, 1 (2007).
- [3] M. D. Gunzburger, J. S. Peterson, and H. Kwon, “An Optimization Based Domain Decomposition Method of Partial Differential Equations”, *Computers and Mathematics with Applications*, **37**, 77 (1999).
- [4] Q. Du and M. D. Gunzburger, “A Gradient Method Approach to Optimization-based Multidisciplinary Simulations and Nonoverlapping Domain Decomposition Algorithms”, *SIAM Journal on Numerical Analysis*, **37**, 1513 (2000).
- [5] W. E, B. Engquist, X. Li, W. Ren, and E. Vanden-Eijnden, “Heterogeneous multiscale methods: A review”, *Communications in Computational Physics*, **2**, 367 (2007).

Approximating the quasicontinuum method using quadrature rules

Yanzhi Zhang^{*}, Max Gunzburger

Department of Scientific Computing, Florida State University,
Tallahassee, FL 32306-4120, USA.

ABSTRACT

A quadrature-rule type approximation to the quasicontinuum method is described. Its computational complexity depends on the number of representative particles but not on the total number of particles. Simple numerical examples are provided to illustrate the accuracy and efficiency of this method.

1 Introduction

Consider a crystal with N particles and let $\mathcal{N} = \{1, \dots, N\}$ denote the index set of all particles. The positions of the particle α in the reference and a deformed configuration are defined by \mathbf{X}_α and \mathbf{x}_α , respectively. In practice, the positions of some particles may be specified, and let $\mathcal{N}_f \in \mathcal{N}$ denote the index set of these particles. Then denote $\mathcal{N}_a = \mathcal{N} \setminus \mathcal{N}_f$ the index set of the remaining unspecified particles. The total potential energy is given by

$$\Phi(\{\mathbf{x}_\alpha\}_{\alpha \in \mathcal{N}}) = \sum_{\alpha \in \mathcal{N}} \sum_{\beta \in \mathcal{N}, \beta > \alpha} \Phi^a(\mathbf{x}_\alpha, \mathbf{x}_\beta) + \sum_{\alpha \in \mathcal{N}} \Phi^e(\mathbf{x}_\alpha), \quad (1)$$

where $\Phi^a(\mathbf{x}_\alpha, \mathbf{x}_\beta)$ denotes the interacting potential between particle α and β , and $\Phi^e(\mathbf{x}_\alpha)$ is the potential due to the external force acting on particle α , which is assumed to be conservative. To determine the stable equilibrium configurations of the crystal, we can minimize the energy (1) with respect to all unspecified particles, equivalently, by solving the problem¹

$$\frac{\partial \Phi}{\partial \mathbf{x}_\alpha}(\{\mathbf{x}_\alpha\}_{\alpha \in \mathcal{N}}) = \mathbf{0} \quad \text{for } \alpha \in \mathcal{N}_a. \quad (2)$$

In general, our aim is not simply to determine the absolute minimizer of $\Phi(\{\mathbf{x}_\alpha\}_{\alpha \in \mathcal{N}})$, but rather the set of metastable configurations of the crystal, which is physically more relevant.

We see that, (2) is a system of² dN_a equations in the dN_a unknowns with N_a of the same order as N . Usually, the number N is huge, which makes it almost impossible to directly simulate this whole system. The quasicontinuum (QC) method using representative particles is one of the most successful multiscale techniques to simplify large atomic systems [1, 2]. However, it still involves calculations over the full atomic lattices so that its complexity depends on the total number of particles [3]. The aim of this paper is to present a quadrature-rule (QC-QR) type approximation to the QC method. It is organized as follows. In Section 2, we review the QC method for molecular statics. Section 3 shows the details of the QC-QR method and numerical experiments. A brief summary is provided in Section 4.

^{*}Email: yzhang@scs.fsu.edu.

¹The notation $\partial \Phi / \partial \mathbf{y}$ denotes the d -vector $\nabla_{\mathbf{y}} \Phi$ having components $\partial \Phi / \partial y_k$, $k = 1, \dots, d$.

² d is the spatial dimension, and N_a denotes the cardinality of the index set \mathcal{N}_a .

2 Quasicontinuum method

To apply the quasicontinuum (QC) method, we start by selecting a reduced set of *representative particles*, and details about it are given in, e.g., [3]. Let $\tilde{\mathcal{N}}_r \subset \mathcal{N}$ denote the index set of the representative particles. Typically, we choose all the specified particles to be among the representative particles, i.e., $\mathcal{N}_f \subset \tilde{\mathcal{N}}_r$, and then let $\mathcal{N}_r = \tilde{\mathcal{N}}_r \setminus \mathcal{N}_f$. Denote $\mathbb{T}_h = \{\Delta_t\}_{t=1}^T$ a triangulation in the reference configuration which consists of simplices having the representative particles as vertices. Let $\mathbb{T}_{h,j} = \{\Delta_t \mid \mathbf{X}_j \in \bar{\Delta}_t\}$ be the set of simplices which have \mathbf{X}_j as a vertex. Denote $\{\psi_j^h(\mathbf{X})\}_{j \in \tilde{\mathcal{N}}_r}$ a basis for the space of continuous, piecewise linear polynomials corresponding to the triangulation \mathbb{T}_h . In particular, we choose the basis so that

$$\psi_j^h(\mathbf{X}_i) = \delta_{ij}, \quad \text{if } i, j \in \tilde{\mathcal{N}}_r \quad \text{and} \quad \psi_j^h(\mathbf{X}) = 0, \quad \text{if } \mathbf{X} \notin \mathbb{T}_{h,j}.$$

By the Cauchy-Born rule, we assume that

$$\mathbf{x}_\alpha^h = \sum_{k \in \tilde{\mathcal{N}}_r} \mathbf{x}_k^h \psi_k^h(\mathbf{X}_\alpha) \approx \mathbf{x}_\alpha \quad \text{for } \alpha \in \mathcal{N}_a, \quad (3)$$

where \mathbf{x}_k^h is the (approximate) position of the representative particle $k \in \tilde{\mathcal{N}}_r$. Denoting $\mathcal{N}_j = \{\alpha \in \mathcal{N}_a \mid \mathbf{X}_\alpha \in \text{supp}(\psi_j^h(\mathbf{X}))\}$, then we have that (2) reduces to

$$\sum_{\alpha \in \mathcal{N}_j} \psi_j^h(\mathbf{X}_\alpha) \left(\sum_{\beta \in \mathcal{N}, \beta \neq \alpha} \mathbf{f}^a(\mathbf{x}_\alpha^h, \mathbf{x}_\beta^h) \right) + \sum_{\alpha \in \mathcal{N}_j} \psi_j^h(\mathbf{X}_\alpha) \mathbf{f}^e(\mathbf{x}_\alpha^h) = \mathbf{0}, \quad j \in \mathcal{N}_r \quad (4)$$

where $\mathbf{f}^a(\mathbf{x}_\alpha, \mathbf{x}_\beta) = -\partial\Phi^a(\mathbf{x}_\alpha, \mathbf{x}_\beta)/\partial\mathbf{x}_\alpha$ denotes the force acting on particle α due to particle β , and $\mathbf{f}^e(\mathbf{x}_\alpha) = -\partial\Phi^e(\mathbf{x}_\alpha)/\partial\mathbf{x}_\alpha$ is the external force.

It is easy to see that the system (4) includes dN_r equations and the same number of degrees of freedom, but the work involved in determining its solution depends on N , the total number of particles. Furthermore, the QC method can not essentially reduce the complexity in computing the total energy (1), which still requires a work of $O(N^2)$.

3 Quadrature-rule type approximations

To mitigate the dependence of the total number of particles in the QC method, we have to approximate all sums appearing in the force balance equations (4) and in the energy (1), i.e., the sums having the form

$$G = \sum_{\alpha \in \mathcal{N}} g(\mathbf{X}_\alpha), \quad G_j = \sum_{\alpha \in \mathcal{N}_j} g(\mathbf{X}_\alpha), \quad \text{and} \quad S_\alpha = \sum_{\beta \in \mathcal{N}} s(\mathbf{X}_\alpha, \mathbf{X}_\beta), \quad (5)$$

where $g(\cdot)$ and $s(\cdot, \cdot)$ are appropriate functions. These sums may be broken into the sums over all representative particles \mathbf{X}_j , $j \in \tilde{\mathcal{N}}_r$, and over all simplices Δ_t , $t = 1, \dots, T$, in the triangulation \mathbb{T}_h . To this end, we denote $\mathcal{N}_t = \{\alpha \in \mathcal{N}_a \mid \mathbf{X}_\alpha \in \Delta_t\}$ as the index set of the particles located inside of the simplex Δ_t . Let $\mathcal{T}_j = \{t \in \{1, \dots, T\} \mid \Delta_t \in \mathbb{T}_{h,j}\}$ denote the index set of the simplices in the support regions of the basis function $\psi_j^h(\cdot)$. Then we get

$$\sum_{\alpha \in \mathcal{N}} = \sum_{t=1}^T \sum_{\alpha \in \mathcal{N}_t} + \sum_{k \in \tilde{\mathcal{N}}_r}, \quad \text{and} \quad \sum_{\alpha \in \mathcal{N}_j} = \sum_{t \in \mathcal{T}_j} \sum_{\alpha \in \mathcal{N}_t} + \sum_{\alpha=j}. \quad (6)$$

We now focus on the inner sums over individual simplices. Choose the subset

$$\mathcal{N}_{t,q} = \begin{cases} \mathcal{N}_t & \text{if } N_t \leq q \\ \text{a } q\text{-dimensional subset of } \mathcal{N}_t & \text{otherwise,} \end{cases} \quad (7)$$

i.e., $\mathcal{N}_{t,q}$ consists of at most q particles chosen from among the particles in the simplex Δ_t . Then the inner sums in (6) can be approximated by

$$\sum_{\alpha \in \mathcal{N}_t} g(\mathbf{X}_\alpha) \approx \sum_{\beta \in \mathcal{N}_{t,q}} \omega_{t,\beta} g(\mathbf{X}_\beta). \quad (8)$$

Combining (6) and (8), we can easily get the approximations to the sums G and G_j . Since the function $s(\cdot, \cdot)$ in S_α depends on the relative positions of two particles, we can not simply apply (8) to the sums S_α , and we have the following two cases:

In a short-range interaction case, the particle only interacts with its nearby particles, so we can assume that $\Phi^a(\mathbf{x}_\alpha, \mathbf{x}_\beta) = 0$, when $|\mathbf{x}_\beta - \mathbf{x}_\alpha| > r$ for some $r > 0$. Denote $\mathcal{N}_{\alpha,r} = \{\beta \in \mathcal{N} \mid 0 < |\mathbf{x}_\beta - \mathbf{x}_\alpha| \leq r\}$ the index set of the particles interacting with the particle α . Then the sums S_α can be reduced to

$$S_\alpha = \sum_{\beta \in \mathcal{N}} s(\mathbf{X}_\alpha, \mathbf{X}_\beta) \approx \sum_{\beta \in \mathcal{N}_{\alpha,r}} s(\mathbf{X}_\alpha, \mathbf{X}_\beta). \quad (9)$$

While for the long-range case, the particle interacts with all particles, but the interaction becomes weaker when the distance between two particles increases. Thus we can denote $\mathcal{T}_{\alpha,r} = \{t \in \{1, \dots, T\} \mid d(\Delta_t, \mathbf{X}_\alpha) < r\}$ the index set of simplices whose distance to the particle α is less than r units, where the distance between a simplex Δ_t and a particle \mathbf{X}_α is defined by $d(\Delta_t, \mathbf{X}_\alpha) = \min_{\beta \in \mathcal{N}_t} |\mathbf{X}_\beta - \mathbf{X}_\alpha|$. Then the sum S_α is approximated by

$$S_\alpha \approx \sum_{t \in \mathcal{T}_{\alpha,r}} \sum_{\beta \in \mathcal{N}_t} s(\mathbf{X}_\alpha, \mathbf{X}_\beta) + \sum_{t \notin \mathcal{T}_{\alpha,r}} \sum_{\beta \in \mathcal{N}_{t,q}} \omega_{t,\beta} s(\mathbf{X}_\alpha, \mathbf{X}_\beta) + \sum_{k \in \tilde{\mathcal{N}}_r} s(\mathbf{X}_\alpha, \mathbf{X}_k). \quad (10)$$

The selection of ‘‘quadrature’’ points \mathbf{X}_β and computation of $\omega_{t,\beta}$ are done in the reference configuration, and they can be used for all the steps of an iterative solution process.

To test the performance the quadrature-rule type method, we use a simple one-dimensional particle chain with $N = 4096$ particles as our example. The potentials are chosen as

$$\Phi^a(r) = 4\epsilon_0 \left[\left(\frac{\sigma}{r}\right)^{12} - 2 \left(\frac{\sigma}{r}\right)^6 \right] + \frac{1}{4\pi\epsilon_1} \frac{q_\alpha q_\beta}{r}, \quad \phi^e(\mathbf{x}) = \frac{1}{100\mathbf{X}_N} \left(\frac{\mathbf{X}_N}{2} - \mathbf{x} \right)^2, \quad (11)$$

where $r = |\mathbf{x}_\alpha - \mathbf{x}_\beta|$ and \mathbf{X}_N is the position of the right-most particle in the reference configuration. The parameters are chosen as $\epsilon_0 = \sigma = 1$, $\epsilon_1 = 0.01$ and $q_\alpha = +1$ for $\alpha \in \mathcal{N}$. In the reference configuration, all particles are uniformly distributed with a distance $h = 1$. The left-most and right-most particles are fixed, i.e., $\mathbf{x}_1 = \mathbf{X}_1$ and $\mathbf{x}_{4096} = \mathbf{X}_{4096}$.

Fig. 1 shows the errors of the QC and QC-QR methods by comparing with the full atomistic method. From it, we see that the errors of both methods decrease when the number of representative particles increases. On the other hand, the errors from the QC-QR method are always larger than those from the QC method. This is because the error of the QC-QR method includes: i) the reduction of the number of degrees of freedom from N_a to N_r through the use of the Cauchy-Born rules and the use of representative particles; ii) the use of quadrature-rule type approximation to the sums in the QC method; iii) the ‘truncation’ of the interaction potential. However, from the figure, we see that, for a given error level, the time used by the QC-QR method is usually much shorter than that spent by the QC method.

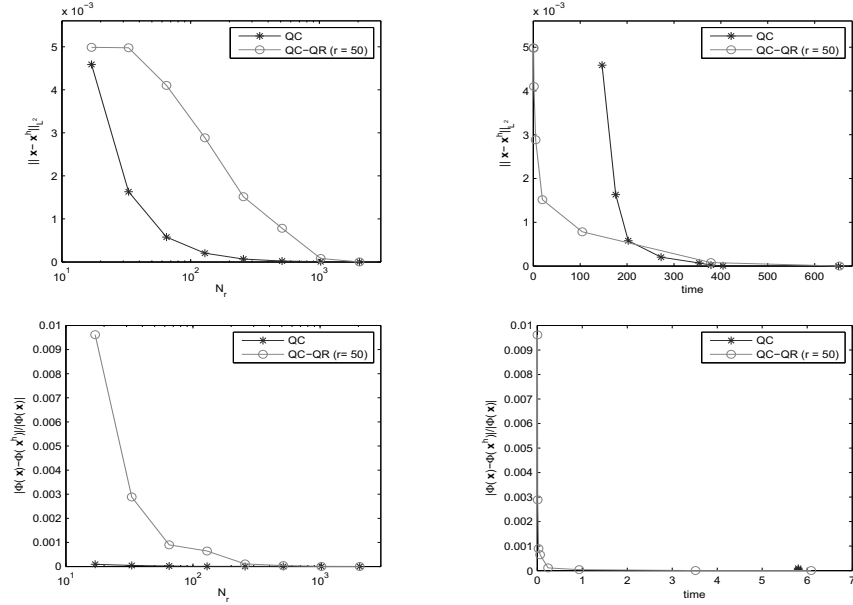


Figure 1: Average position error (up) and relative energy error (down) versus the number of representative particles (left) and computational time (right).

4 Summary

We presented a quadrature-rule (QC-QR) type approximation to the quasicontinuum (QC) method. This method essentially reduces the complexity of the QC method, and its computational cost depends on the number of representative particles. Numerical experiments showed that the QC-QR method has enough accuracy but it is much faster than the QC method. Details about the methods described in this paper may be found in [4, 5]. In the future, a much greater array of tests in two and three dimensions are needed to ultimately provide convincing evidence about the efficacy of the QC-QR methods.

Acknowledgements This work was supported by the Office of Science of the U.S. Department of Energy under grant number DE-FG02-05ER25698.

References

- [1] R. Miller and E. B. Tadmor, “The quasicontinuum method: Overview, applications and current directions”, *Journal of Materials Design*, **9**, 203 (2002).
- [2] Quasicontinuum website: <http://www.qcmethod.com>.
- [3] J. Knap and M. Ortiz, “An analysis of the quasicontinuum method”, *Journal of the Mechanics and Physics of Solids*, **49**, 1899 (2001).
- [4] M. Gunzburger and Y. Zhang, “A quadrature-rule type approximation to the quasicontinuum method”, to appear.
- [5] Y. Zhang and M. Gunzburger, “Quadrature-rule type approximations to the quasicontinuum method for short and long-range interatomic interactions”, to appear.

Analysis of Quasicontinuum Method

Pingbing Ming

**Institute of Computational Mathematics, Chinese Academy of Sciences, Beijing, P.R.
China; mpb@lsec.cc.ac.cn**

ABSTRACT

In this talk, I will report some recent work for the analysis of quasicontinuum method. The stability and accuracy of nonlocal quasicontinuum method with planar interface will be discussed, and extensions to certain force-based methods will also be covered. In particular, we will focus on the ghost-force problem in QC.

This is a joint work of Weinan E in Princeton University and Zhijian(Jerry) Yang in Caltech. This work is supported by National Natural Science Foundation of China under the grant 10571172 and the National Basic Research Program under the grant 2005CB321704

Quadrature and Implementation of the Weak Coupling Method

Authors: K. Fackeldey, D. Krause and R. Krause

Affiliations: Institute for Numerical Simulation, University of Bonn,
Wegelerstrasse 6, 53115 Bonn, Germany, krause@ins.uni-bonn.de.

ABSTRACT

We discuss a new method for coupling molecular dynamics and continuum mechanics, which is based on a function space oriented approach. For this purpose, the micro scale displacements originating from molecular dynamics in the Euclidean space are extended into a Sobolev space using a partition of unity. Then, a scale decomposition is realized in L^2 by means of an orthogonal projection, giving rise to our new weak scale transfer operator in function space. Here, we consider the assembling process of the algebraic representation of this weak coupling operator and show that the assembling can be done in (quasi-)optimal complexity.

1. Introduction

A detailed analysis of nonlinear phenomena in structure mechanics by using molecular dynamics is even with the increasing computational power not always possible. This can be seen as a motivation for mathematical models and simulation methods on a macro scale, like continuum mechanics and the finite element method. For one thing such continuum methods on the coarse scale reduce the computational expense. For the other thing those methods become very challenging when resolving highly nonlinear effects like cracks. It is the basic idea of multiscale methods to combine fine scale simulations with coarse scale simulations in order to exploit the advantages of both methods. In the last decades several approaches have been developed. For an exhaustive overview we refer to [1] and [2]. Here, we discuss the new function space oriented coupling approach [6] with respect to some of its more technical aspects.

2. The Decomposition of Scales

For the derivation of our new weak coupling approach, in a first step, we follow Hughes et al.[3] by applying scale separation techniques. Starting from a total displacement u in the computational domain $\Omega \subset \mathbb{R}^d$, we separate the fine scale parts u' of u from its coarse scale parts \bar{u} by means of the decomposition

$$u = u' + \bar{u} \tag{1}$$

see [3, 4]. In our multiscale context, this decomposition is intended to separate the high oscillatory atomic displacements from the remaining part of the solution on the macro scale. Any scale decomposition in the fashion of (1) has to deal with the difficulty that using molecular dynamics on the micro scale, for N atoms, the displacements are given as point-values in the "discrete", i.e., finite dimensional, space \mathbb{R}^{dN} ; in contrast, the

macro scale displacements are usually assumed to be some functions, e.g., elements of the Sobolev space. Thus, in order to formulate the scale decomposition (1) properly, a suitable space has to be chosen, which contains the atomistic displacements as well as the macro scale displacements.

3. The Weak Coupling Concept

As afore mentioned, the displacements generated by molecular dynamics are given in the Euclidean space as scattered data

$$\chi_N = \{(X_\alpha, \nu_\alpha) : \alpha = 1, \dots, N; X_\alpha \in \Omega \subset \mathbb{R}^d; \nu_\alpha \in \mathbb{R}^d\}.$$

However, since we attempt to perform a scale separation in the spite of [3, 4], we employ a mapping $\iota : \chi_N \rightarrow L^2(\Omega)$, transferring the molecular displacements into function space. The construction of such a mapping is not an easy task at all. Here, we use techniques from scattered data approximation to construct a Partition of Unity (see, e.g., [5]). For each particle, we choose a weight function

$$W_\alpha : \mathbb{R}^d \rightarrow \mathbb{R} \text{ with } \text{supp}(W_\alpha) = \omega_\alpha \text{ such that } \bigcup_\alpha \omega_\alpha \supset \Omega \quad (2)$$

We refer to [6] for a more detailed explanation of this process. As a consequence, the resulting micro scale displacement can be expressed as

$$u(x) = \sum_\alpha \nu_\alpha \varphi_\alpha(x) \text{ where } \varphi_\alpha(x) = \frac{W_\alpha(x)}{\sum_\beta W_\beta(x)}. \quad (3)$$

In order to identify the coarse scale displacement, we employ an L^2 - projection onto the finite element space $S^h(\Omega) = \text{span}\{\lambda_p\}_{p \in N^h}$. More precisely, the coarse scale displacement is given by

$$\pi : L^2(\Omega) \rightarrow S^h(\Omega), \quad (\pi(w), \mu)_{L^2(\Omega)} = (w, \mu)_{L^2(\Omega)} \text{ for all } \mu \in M^h \quad (4)$$

Here, $M^h = \text{span}\{\mu_p\}_{p \in N^h}$ is a multiplier space which needs to fulfill an inf-sup condition. In [6], different choices for the multiplier space are discussed. The algebraic representation of (4) is given by

$$\pi(w) = M^{-1}Rw,$$

where we have identified $\pi(w)$ and w with their respective coefficients. For the first matrix R , we need to evaluate integrals of the form $R_{p\alpha} = \int \mu_p \varphi_\alpha$. The matrix M with entries $M_{qp} = \int \lambda_q \mu_p$ has the character of a finite element mass matrix.

4. Implementation

The assembling of the transfer operator in dimensions $d \geq 2$ is a subtle task. Due to the large number of atoms in Ω we are in need for an efficient, yet robust, algorithm for the

construction of the algebraic representation of π . Since the assembling of the rectangular matrix R requires the computation of all intersections $\omega_\alpha \cap t$, $t \in T^h$, T^h being the set of all elements in the finite element mesh, we have chosen rectangular/cuboid patches ω_α (see [5]). In the engineering literature, often radial patches are used in connection with a fixed background mesh for the quadrature. This allows for the use of radial basis functions φ_α which is mathematically very appealing. However, exact integration with a background mesh and standard quadrature formulas (such as Gauss-Christoffel) is almost impossible. Rectangular patches allow for exact quadrature, which is needed for the stability of $M^{-1}R$. Furthermore, the computation of the cuts $\omega_\alpha \cap t$ can be handled by using ideas from computational geometry as described below. For representing the projection π we need to assemble the matrices M and R . The assembling of M and R is similar, even though for special choices of M^h the computation of M is simpler (e.g., if $M^h = S^h$).

For the efficient implementation of the assembling we need to perform the following tasks with (quasi-)optimal complexity:

1. Given a finite element mesh-element $t \in T^h$ find all atoms α such that $\omega_\alpha \cap t \neq \emptyset$.
2. Compute the polytope $\omega_\alpha \cap t$.
3. Decompose $\omega_\alpha \cap t$ into simpler polytopes on which quadrature formulas for the exact integration can be applied.

Step 1 is closely related to the construction of the patches ω_α . In [5], tree-based algorithms for the Partition of Unity Method (PUM) are introduced. However, the main drawback in our application is that they require the introduction of new (artificial) points/patches, see (2). For lattice systems however the overlap property (2) can be easily guaranteed for suitably chosen sizes of $\text{diam}(\omega_\alpha)$. The use of an quadtree (octree) or kd-trees structure yields quasi-optimal complexity for queries as in Step 1. For the cut-computations in Step 2 we apply the quickhull algorithm [7] along with a simplex method. For each cut $\omega_\alpha \cap t$ we need to compute an interior point. This is realized by describing each cut $\omega_\alpha \cap t$ as the intersection of finitely many halfplanes $\{x \in \mathbb{R}^d \mid -n_j^T x + d_j \geq 0, j = 1, \dots, n\}$. For $d = 3$, after the introduction of the two additional variables x_4, x_5 , an interior point $(p_1, p_2, p_3)^T = \left(\frac{x_1}{x_4}, \frac{x_2}{x_4}, \frac{x_3}{x_4}\right)^T$ can be obtained from the linear constrained maximization problem:

Maximize x_5 among all tuples $(x_1, x_2, x_3, x_4, x_5)$ such that

$$-n_j^T(x_1, x_2, x_3)^T + d_j \cdot x_4 - x_5 \geq 0, j = 1, \dots, n$$

and $x_5 > 0, x_4 \geq \varepsilon$ with small $\varepsilon > 0$.

Given such an interior point, the intersection algorithm from [8] is applied, which gives a description of $\omega_\alpha \cap t$ by means of halfplanes.

In case of sufficiently smooth basis functions, i.e. $\varphi_\alpha \in C^1$, Step 3 could be carried out by computing a Delaunay triangulation of the polytope $\omega_\alpha \cap t$ and applying a quadrature formula of sufficient high order on each triangle/tetrahedron. However, in our application $\varphi_\alpha \in C^1$ generally is not fulfilled, for the following two reasons:

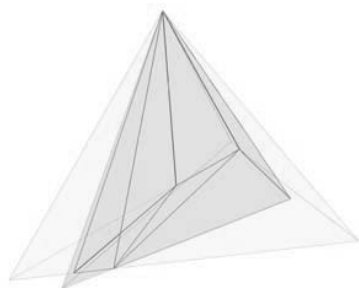


Figure 1: Two tetrahedra in \mathbb{R}^3 and Delaunay triangulation of the resulting cut polytope

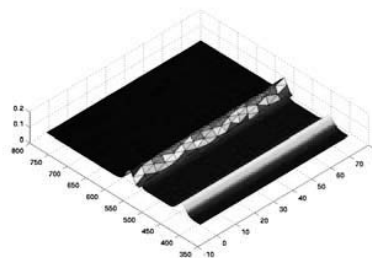


Figure 2: Example of a coupled simulation with the weak coupling method in $2d$: transfer of a wave from micro to macro

- The functions W_α are constructed from one-dimensional splines by a tensor-approach. For linear splines, a jump in the derivatives along the connections between the center of mass of ω_α and the midpoints of the edges/sides occurs.
- Even for smooth functions W_α , the derivative of φ_α can be discontinuous along $\omega_\alpha \cap \partial\omega_\beta$, $\alpha \neq \beta$ and $\omega_\alpha \cap \omega_\beta \neq \emptyset$.

As a consequence, for the assembling of R the set $D_{\alpha,t} = \{x \in t : \nabla\varphi_\alpha \text{ discontinuous in } x\}$ needs to be resolved for each $t \in T^h$. This can be done by either choosing a Delaunay triangulation which conforms to the constraint that $D_{\alpha,t}$ is contained in the union of all edges/sides, or by subdividing ω_α prior to the cut detection and applying Step 2 and Step 3 to each sub-rectangle/sub-cuboid separately.

References

- [1] W.A. Curtin and R.E. Miller, "Atomistic/continuum coupling in computational materials science", *Mod. Sim. Mat. Sci. Eng.*, 11, R33-R68, 2003
- [2] W. E, B. Engquist, X. Li, W. Ren and E.V. Eijnden, "The heterogeneous multiscale method: a review", *Comm. Math. Sci.*, 1(1): 87-132, 2003
- [3] T. Hughes, G. Feijoo, J. Mazzei and J. Quincy, "The variational multiscale method - a paradigm for computational mechanics", *Comp. Meth. Appl. Mech.*, 166, 3-24, 1998
- [4] G.J. Wagner and W.K. Liu, "Coupling of atomistic and continuum simulations using a bridging scale decomposition", *J. Comp. Phys.*, 190, 249-274, 2003
- [5] M. A. Schweitzer, "A parallel multilevel partition of unity method for elliptic partial differential equations", *LNCSE Springer*, 29, 2003
- [6] K. Fackeldey and R. Krause "Multiscale coupling in function space - weak coupling between Molecular dynamics and continuum mechanics", *SFB 611, Preprint 350*, 2007
- [7] C. M. Barber, D. P. Dobkin, and H. Huhdanpaa. "The quickhull algorithm for convex hulls". *ACM Trans. Math. Softw.*, 22(4):469-483, 1996.
- [8] F. Preparata and M. Shamos, "Computational Geometry", Springer, New York, 1985

Peridynamics, Molecular Dynamics, and Classical (nonlinear) Elasticity

Richard Lehoucq, Stewart Silling

**Sandia National Laboratories, Albuquerque, NM 87185-1322, USA
(E-mails: rblehou@sandia.gov, sasilli@sandia.gov)**

ABSTRACT

My presentation describes peridynamics (Silling 2000) as a continuum limit of molecular dynamics. Peridynamics uses a nonlocal force interaction, and does not make any assumptions (e.g. continuity) on the displacement field in contrast to classical elasticity. Under the assumption of a smooth deformation, a theorem is presented that demonstrates that as the horizon defining the nonlocal force interaction decreases, the peridynamic equation of motion converges to the classical (nonlinear) elastic equation of motion.

Molecular dynamics at Larger Scales: Peridynamics as an upscaling of molecular dynamics

Michael L. Parks¹, Pablo Seleson²

¹**Applied Mathematics and Applications, Sandia National Laboratories, P.O. Box 5800, MS 1320, Albuquerque, NM 87185 (E-mail: mlparks@sandia.gov)**

²**Dept. of Scientific Computing, 400 Dirac Science Library Florida State University Tallahassee, FL 32306-4120 (E-mail: seleson@scs.fsu.edu).**

ABSTRACT

The peridynamic model is a reformulation of solid mechanics based on integral equations. It is a nonlocal model, accounting for the effects of long-range forces. Correspondingly, classical molecular dynamics is also a nonlocal model. Peridynamics and molecular dynamics have similar computational structures, as both methods compute the forces on a particle by summing the forces from surrounding particles. The peridynamic model can be shown under certain assumptions to converge to the classical equation of elasticity [1, 2]. Likewise, certain particle models can be upscaled to the classical equation of elasticity [3]. We will concern ourselves with the length scales between those of molecular dynamics and classical elasticity, and explore how the peridynamic model can be cast as an upscaling of molecular dynamics. Specifically, we address the extent to which the solutions of molecular dynamic simulations can be recovered by a peridynamic model.

[1] E. Emmrhc and O. Weckner, “On the Well-Posedness of the Linear Peridynamic Model and its Convergence Towards the Navier Equation of Linear Elasticity”, *Communications in Mathematical Sciences*, **5**, 851 (2007).

[2] S. Silling and R. Lehoucq, “Convergence of Peridynamics to Classical Elasticity Theory”, *Journal of Elasticity*, in press, (2008).

[3] M. Arndt and M. Griebel, “Derivation of Higher Order Gradient Continuum Models from Atomistic Models for Crystalline Solids”, *Multiscale Modeling and Simulation*, **4**, 531 (2005).

Sandia is a multiprogram laboratory operated by Sandia Corporation, a Lockheed Martin Company, for the United States Department of Energy under contract DEAC04-94AL85000.

Coarse-graining the Free energy of Atomistic Systems: a simple case

Xavier Blanc^{1,2}, Claude Le Bris^{3,2}, Frédéric Legoll^{4,2}, Carsten Patz⁵

¹Laboratoire J.-L. Lions, Université Pierre et Marie Curie, Boite courrier 187, 75252 Paris Cedex 05, France (E-mail: blanc@ann.jussieu.fr)

²INRIA Rocquencourt, MICMAC team-project, Domaine de Voluceau, BP 105, 78153 Le Chesnay Cedex, France

³CERMICS, Ecole Nationale des Ponts et Chaussées, 6 et 8 avenue Blaise Pascal, 77455 Marne-la-Vallée Cedex 2, France (E-mail: lebris@cermics.enpc.fr)

⁴LAMI, Ecole Nationale des Ponts et Chaussées, 6 et 8 avenue Blaise Pascal, 77455 Marne-la-Vallée Cedex 2, France (E-mail: legoll@lami.enpc.fr)

⁵Weierstrass-Institut für Angewandte Analysis und Stochastik, Mohrenstrasse 39, 10117 Berlin, Germany (E-mail: patz@wias-berlin.de)

ABSTRACT

Molecular dynamics is a classical method to compute constant temperature thermodynamical averages. For instance, the evolution of a material science system according to the Langevin equation is simulated, while some relevant observables are averaged along the trajectory. It is often the case that interesting observables actually do not depend on all the particles, but only on the position of some of them, called repatoms, in the QuasiContinuum terminology. In this case, it is natural to try and design a strategy to compute more efficiently the canonical averages under study. The free energy of the coarse-grained model is another interesting quantity, which leads to the constitutive relation of the material, at a given temperature. In this talk, we will consider a 1D chain of atoms, and we present a rigorous and efficient method to compute ensemble averages and free energies, based on a thermodynamic limit procedure [1]. We consider the NN and the NNN cases and illustrate the obtained theoretical results with numerical simulations. Our strategy also applies to chain-like materials, such as polymers.

- [1] X. Blanc, C. Le Bris, F. Legoll, C. Patz, “Finite-temperature Coarse-graining of One-dimensional Models: Mathematical Analysis and Computational Approaches”, INRIA preprint RR-6544 (may 2008), available at <http://hal.inria.fr/inria-00282107/en/>.

Inverse Microstructure Design Based on Statistical correlation functions

Hamid Garmestani

**Materials Science and Engineering, Georgia Institute of Technology, Atlanta, GA, USA;
(E-mail: hamid.garmestani@mse.gatech.edu)**

ABSTRACT

Inverse computational design of materials is a formidable task requiring solutions to strongly coupled properties and constraints and direct linkage to microstructure. The resulting coupled field equations for these problems can be solved using Green's function's formulations, and the properties and constraints linked to the microstructure using statistical correlation functions. However, a rigorous link between statistical continuum mechanics relations and properties requires a complete representation of microstructure using n-point correlation functions and Green's functions formulations to the solution of field equations. While many materials properties are often modeled by their ensemble averages, other properties (eg. fracture, fatigue) strongly relevant for their performance in structural applications are affected by the tails of the distribution functions. Statistical representation of microstructures using higher order correlation functions within the statistical continuum mechanics framework can provide a direct mathematical link between microstructure and properties (and constraints). Such a linkage is also an important tool for inverse computational materials design. Not only can it provide the properties from any set of microstructures within the material's Hull, but the linkage can allow us to find microstructures that meet the designer's specifications and requirements. The output of the inverse design is then the set of higher order probability distributions functions that represent the optimum microstructure. This makes the task of reconstruction and realization of realistic microstructures from the set of statistical correlation functions another computational and mathematical challenge in the process. Several methodologies have been developed to accomplish this task and more work is needed to develop more efficient algorithms that can address the contribution from higher order functions.

A Review of Recent Transition State Search Methods in Phase Transition Simulation

Yan Wang¹, Vernet Lasrado¹, and Devendra Alhat²

¹University of Central Florida, Orlando, Florida 32816, USA; ²Indian Institute of Technology-Bombay, Mumbai 400076, India.
(E-mail: wangyan@mail.ucf.edu)

ABSTRACT

In this paper, a review of recent methods to search for transition states on a potential energy surface that characterize phase transitions is given. Finding the saddle point(s) and the minimum energy path on a complex potential energy surface is the major challenge to accurately simulate the kinetics of chemical reactions and phase transitions. Once the saddle points have been identified and the activation energy for the transition is known, one can apply methods such as kinetic Monte Carlo and accelerated molecular dynamics to simulate the transition process. The transition state searching methods are categorized into two groups, minimum energy path search and saddle point search. We primarily summarize the methods developed in the last two decades.

1. Introduction

A phase transition is a geometric and topological transformation process of materials from one phase to another, each of which has a unique and homogeneous physical property. In an effort to simulate a reaction or transition, a potential energy surface (PES) that characterizes the process is first generated. Then, a minimum energy path (MEP) is computed which represents the transition pathway in the configuration space. With knowledge of the activation energy, the rate constant that defines the speed of the process then can be calculated using transition state theory (TST). Finally, the reaction or transition can be simulated by methods such as kinetic Monte Carlo and accelerated molecular dynamics. The most important step involved in modelling phase transition is the knowledge of the activation energy barrier and rate constant involved in the transition. Various numerical methods to search transition paths and saddle points have been developed. Some review papers [1,2,3] were published. However, there have been new methods and improvements that have yet to be documented. This paper gives a brief summary of these latest advancements without listing references due to the page limit. Interested readers are referred to [4,5] for more detailed reviews and references of the methods discussed.

We categorize the computational modelling methods into two types: transition path search and saddle point search. Transition path search methods generate the MEP on the PES, whereas saddle point search methods aim at finding the saddle points on the PES. In the rest of the paper, we summarize transition path search methods in Section 2 and saddle point search methods in Section 3 respectively.

2. Transition Path Search Methods [4]

2.1 Chain-of-States Methods

In chain-of-states methods, the transition pathway is represented as a number of intermediate states, which can be looked at as snapshots of the atomic configurations as the atomic structure transforms from initial to final state along the transition pathway. Usually it requires that the initial and final states should be known. After the search converges, the discrete states are chained to each other, usually by interpolating between the states, to obtain the transition pathway and saddle points. They work well in transitions where there may be more than one saddle point. In situations where there may be multiple transition pathways, the methods will converge to the one that is closest to the initial guess for the pathway.

The nudged elastic band (NEB) method and its extensions are among the most used and well-developed chain-of-states methods. The NEB is an extension of the plain elastic band (PEB) method, where images, which are points in the configuration space corresponding to intermediate states, are connected by springs. In PEB, images move according to both the true force due to the gradient of potential energy and the spring force. The relaxed band should converge to the MEP. However, when the spring constant is large enough, the perpendicular components of spring forces (with respect to the direction of path) pull images away from saddle points at sharp turns of the path. This *corner cutting* makes PEB overestimate the saddle point energy. On the other hand, when the spring constant is small, the parallel components of true forces make images slide down towards the minima. This *sliding down* reduces the resolution of the region of interest (ROI) near the saddle point. The NEB method is targeted to solve the problems of corner cutting and sliding down by removing the perpendicular component of spring force and the parallel component of true force in the total force on each image. The only effect of springs now is to keep images evenly distributed within the path. Nevertheless, when the potential energy changes rapidly, the path has kinks where the parallel component of the energy gradient is much larger than the perpendicular one, because the restoring perpendicular components of forces are weak. Another shortcoming of NEB is that the actual saddle point may not be located by one of the images directly. Further extensions of the NEB method try to resolve these issues.

The improved tangent NEB (IT-NEB) method reduces the chances of getting kinks by better estimating the tangent direction of the path to approximate MEP at each image. Instead of the central finite difference approximation between one image and its two neighbours as in the original NEB method, only one neighbour is used for tangent estimation in IT-NEB. The climbing image NEB (CI-NEB) method was further developed so that the image with the highest energy actively climbs up to locate the actual saddle point. An alternative to resolve the issue of kinks is the doubly nudged elastic band (DNEB) method where a manipulated perpendicular component of spring force is introduced back into the total force such that the MEP can be restored. To locate the actual saddle points, the eigenvector following (EF) optimization approach can be applied to the result of NEB. To increase the resolution of ROI, adaptive spring constants can be used based on energy levels or gradients. A free end NEB (FENE) method was proposed to keep one end of the band free so that it can swing at a fixed energy level, thus the number of images can be reduced while still maintaining enough resolution. Similar to the String method, Spline-based interpolation was also introduced into the NEB method extension.

The second group of chain-of-states methods is the String methods. The transition path is represented continuously as Splines. Subject to perpendicular forces, the curve evolves and converges to the MEP alternately in two steps: in the evolution step, the curve is discretized as a string of points and solved by standard ODE solvers; in the reparameterization step, the points are redistributed along the string based on parameterization constraints and Spline interpolations. Compared to the NEB methods, where the number of images is fixed during searching, the number of points in the String method can be dynamically modified. The growing String method is an extension where the points of strings are initially located at the two ends of reactant and product. Then the string grows by inserting new points so as to meet at the saddle point upon convergence. The quadratic String method is formulated based on a multi-objective optimization approach. Based on the local quadratic approximation of the PES, the quasi-Newton technique is applied to search the MEP.

2.2 Other Methods

In the conjugate peak refinement (CPR) method, saddle points and the approximated MEP are found by searching the maximum of one direction and the minima of all other conjugate directions iteratively, because exactly one eigenvalue of the Hessian matrix at the saddle points is negative. The accelerated Langevin dynamics (ALD) method is a stochastic transition path sampling method. Paths are sampled by solving the modified Langevin equation with negative friction coefficients to accelerate the transition. The MEP then is the average of all sampled paths. In the concerted variational strategy (CVS) method, the transition motion is described as actions based on the Maupertuis' and Hamilton's principles in classical mechanics, which are integral instead of differential equations. Trajectories have a plane wave representation instead of regular polynomials. The resulted transition trajectory reflects thermal behaviors instead of a smooth MEP curve. The Hamilton-Jacobi (HJ) method generates the MEP by solving a Hamilton-Jacobi type equation with special cost functions.

3. Saddle Point Search Methods [5]

3.1 Local Search Methods

The automated surface walking algorithm is one of the original saddle point search methods. With local quadratic approximations of PES, the search is based on eigenvectors of the Hessian matrix, which is updated iteratively similar to the quasi-Newton technique. It also involves the scaling of one of the active coordinates in order to make the Hessian eigenvalues lie in a required range. In the partitioned rational function optimization method, PES is approximated by rationalized quadratic surfaces, and the search is conducted by partitioning the minimax problem into two separate maximization and minimization subproblems.

More recently, the ridge method searches the saddle point by travelling down along the ridge with a pair of images. The direction of the connecting line between the two images can be constrained to make sure the pair is kept on the ridge. Similarly, the dimer method searches the saddle point based on a pair of images. However, the small distance between the two images is fixed. Starting from one basin, the dimer moves uphill in the translation step. In the rotation step, it rotates towards the lowest curvature mode of PES by minimizing the dimer energy through the

conjugate gradient approach. Later in the improved dimer method, the curvature is calculated differently with reduced numbers of gradient calculations to improve the performance and robustness under numerical noises. In the synchronous transit method, the transition state is initially estimated by minimizing the interpolated inter-atomic distances. Then the saddle point estimate is further refined by employing the conjugate gradient optimization method. In the reduced gradient following method and the reduced potential energy surface model method, stationary points are intersections of zero-gradient curves and surfaces respectively with distinguished coordinates removed. Saddle point search is within the subspace of these zero-gradient curves or surfaces.

3.2 Global Search Methods

Different from local search, the global search methods ensure the saddle point with the maximum energy is located if the search converges to one. The DHS method searches the saddle point by iteratively reducing the distance between reactant and product images while minimizing the energy subject to the equal distance constraint at each step. The Activation-Relaxation Technique searches saddle points in two steps. In the activation step, one image jumps from a local minimum towards a saddle point according to a controlled force. In the relaxation step, it moves from the saddle point to another minimum. Thus it can traverse many saddle points without the knowledge of final product. In the Step and Slide method, the energy levels of two images from the initial and final states are gradually increased. Then the distance between the two is minimized while both images are kept in the same isoenergy surfaces. The interval Newton's method finds all stationary points by solving the equation of vanishing gradient.

Acknowledgements

This work is supported in part by the NSF grant CMMI-0645070.

References

- [1] G. Henkelman, G. Johansson, and H. Jonsson, "Theoretical Methods in Condensed Phase Chemistry", Vol. 5 of *Progress in Theoretical Chemistry and Physics*, Springer, Netherlands, Ch. 10, 269-302 (2002).
- [2] H. Schlegel, "Exploring Potential Energy Surfaces for Chemical Reactions: An Overview of Some Practical Methods", *J. Comp. Chem.*, **24**, 1514-1527 (2003).
- [3] R. Olsen, G. Kroes, G. Henkelman, A. Arnaldson, and H. Jonsson, "Comparison of Methods for Finding Saddle Points without Knowledge of the final states", *J. Chem. Phys.*, **121**, 9776-9792 (2004).
- [4] V. Lasrado, D. Alhat, and Y. Wang, "A Review of Recent Phase Transition Simulation Methods: Transition Path Search," Proceedings of ASME IDETC/CIE2008, Paper No. DETC2008-49410 (2008).
- [5] D. Alhat, V. Lasrado, and Y. Wang, "A Review of Recent Phase Transition Simulation Methods: Saddle Point Search," Proceedings of ASME IDETC/CIE2008, Paper No. DETC2008-49411 (2008).

Finite Element Heterogeneous Multiscale Method and Micromagnetism

Valdemar Melicher, Jan Busa

**Ghent University, Belgium
(E-mail: valdemar.melicher@ugent.be)**

ABSTRACT

We study finite element heterogeneous multiscale method for the Gilbert's equation, the governing equation of dynamic micromagnetism. We consider its form $[\partial_t m = m \times \Delta m - \alpha \partial_t m]$, where m is the magnetisation and α is the damping factor, expressing the magnitude of dissipation in the system. We construct the corresponding compression and reconstruction operators and study their properties.

Homogenization of Stochastic Fractal Microstructures

R.C. Picu,¹ M.A. Soare²

¹Department of Mechanical, Aerospace and Nuclear Engineering, Rensselaer Polytechnic Institute, Troy, NY 12180 (E-mail: picuc@rpi.edu);

²Division of Engineering, Brown University, Providence, RI 02912, (E-mail: Monica_Soare@brown.edu).

ABSTRACT

Many materials with heterogeneous multiscale fractal structure are found in nature. Examples include biological tissues and bone, some rock such as sandstones, and aero-gels. In such materials the amount of geometrical detail observed in the microstructure increases from scale to scale in a self-similar manner, they lack characteristic length scales and the Hausdorff dimension is smaller than that of the embedding space. They are the prototypical examples of problems without scale decoupling. Furthermore, the microstructure is multiscale and stochastic, in the sense that the generating operators that map the geometry from one scale to the next are stochastic. In this work [1], we develop a method by which boundary value problems can be solved for these complex multiscale materials with minimal computational effort. Use is made of the scaling properties of the geometry and of stochastic finite elements in which the solution is approximated using chaos polynomials. The talk will review the formulation and a number of examples used for verification.

[1] M.A. Soare, R.C. Picu, "Boundary value problems defined on stochastic self-similar multiscale geometries," *International Journal for Numerical Methods in Engineering*, **74**, 668 (2008).

Finite Element Methods for a Peridynamic Model of Mechanics

Xi Chen and Max Gunzburger

Department of Scientific Computing

Florida State University

Tallahassee FL 32306-4120

xichen@scs.fsu.edu and gunzburg@scs.fsu.edu

Abstract

Peridynamics is a recently developed theory of solid mechanics that replaces the partial differential equations (PDE) of the classical continuum theory with integro-differential equations (IDE). We apply Finite Element Methods (FEM) to implement the peridynamic model. Since the integro-differential equations remain valid in the presence of discontinuities such as cracks, the method has the potential to model fracture and damage with great generality. We use piecewise constant functions in regions where discontinuities may appear and piecewise linear function in areas where the solutions is smooth and investigate how to combine these two methods. We are also interested in the choice of the horizon radius to implement the peridynamic model more accurately. Theoretical analysis and numerical results for different cases are given.

Key words: peridynamics, finite element methods, integro-differential equations

This work was supported by the Office of Science of the U.S. Department of Energy under grant number DE-FG02-05ER25698.

Bridging Methods and Boundary Treatment for AtC Coupling Problems*

Pablo Seleson¹ and Max Gunzburger²

**Department of Scientific Computing, 400 Dirac Science Library, Florida State University,
Tallahassee, FL 32306-4120, ¹seleson@scs.fsu.edu, ²gunzburg@scs.fsu.edu**

ABSTRACT

We investigate several issues connected with bridging methods for AtC coupling. We study different coupling approaches, using various blending models, as well as the influence of the parameters of the models on the results. One approach we focus on is the use of the Lagrange multiplier method for enforcing constraints on the atomistic and continuum displacements in the bridge region. In addition, we investigate a multiple-neighbor interaction, applying a number of boundary treatments in the atomistic region.

1. Introduction

Atomistic models are computationally too expensive, but continuum models are not accurate enough for describing singular phenomena such as point loads, cracks, etc. For that reason, there is a need of combining atomistic and continuum models. In the Atomistic to Continuum (AtC) coupling technique, we implement a heterogeneous domain decomposition, i.e. the continuum model is applied to part of the domain where an average description of the system is sufficient, while the atomistic description is implemented on other regions, where microscale behavior analysis is needed. The main question arising is how to couple between the different regions, taking into account the different nature of the models implemented on each one. In [1] and [2], a force-based blending model is applied to couple between the atomistic and the continuum models, and an interface region is used to constrain the atomistic displacements by the interpolation of the continuum approximation. In this paper, we follow a similar approach as in [3], using the Lagrange multipliers method to impose the constraints, reducing the number of constraints equations. In contrast to [1], we blend the models at the energy level, and use the potential energy minimization technique to find the equilibrium configuration of our system.

Another issue of interest is the treatment of boundary conditions in the atomistic region. In physical systems, the interaction in the general case is of long-range type, thus a multiple-neighbor interaction has to be implemented in order to get a correct approximation to a real interaction. This brings out a difficulty in relation to the boundary of the system where only a few atoms appear close to the boundary. Therefore, an appropriate treatment is needed in order to correctly describe the system interactions around the boundary. We study several different boundary treatments for multiple-neighbor interactions in the atomistic region.

*This work was supported by the Office of Science of the U.S. Department of Energy under grant number DE-FG02-05ER25698.

2. The Model

The present model combines atomistic and continuum expressions, using blending functions to determine the contribution of each of the representations in each region to the global potential energy. We divide our domain in three regions: Ω_0^C the continuum region, Ω_0^M the atomistic region, and $\Omega_0^{int} = \Omega_0^M \cap \Omega_0^C$ the blending interface for the continuum and the atomistic representations. An illustration of our domain, assuming $\Omega_0^M = [X_i, c]$, $\Omega_0^C = [a, X_f]$, and $\Omega_0^{int} = [a, c]$, is presented in Fig 1.

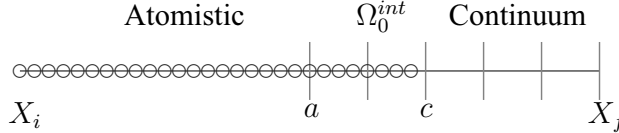


Figure 1: 1-D representation of the domain decomposition. The red lines represent the F.E. nodes, and the blue circles the atomistic particles.

The total potential energy of the system is written as $W = W^{int} - W^{ext}$, where the internal potential energy of the system

$$W^{int} = \int_{\Omega_0^C} \xi(\mathbf{X}) w_C(\mathbf{F}) d\Omega_0^C + \frac{1}{2} \sum_I \sum_J \theta_{I,J} w_M(\mathbf{x}_I, \mathbf{x}_J) \quad (1)$$

and the external potential energy of the system

$$W^{ext} = \int_{\Omega_0^C} \xi(\mathbf{X}) \mathbf{B} \cdot \mathbf{u} d\Omega_0^C + \int_{\Gamma_0^C} \xi(\mathbf{X}) \mathbf{T} \cdot \mathbf{u} d\Gamma_0^C + \sum_I \theta(\mathbf{X}_I) \mathbf{f}_I^{ext} \cdot \mathbf{d}_I \quad (2)$$

with $w_M(\mathbf{x}_I, \mathbf{x}_J)$ the potential energy of the atomistic bond I - J , $w_C(\mathbf{F})$ the potential energy density of the continuum (as a function of the deformation gradient \mathbf{F}), $\mathbf{x}_I = \mathbf{X}_I + \mathbf{d}_I$ the position of the particle I in the current configuration, with \mathbf{d}_I the displacement of the particle I from its position in the reference configuration \mathbf{X}_I , \mathbf{u} the continuum displacement, \mathbf{f}_I^{ext} the external force applied on the particle I , Γ_0^C the boundary of Ω_0^C , \mathbf{B} the external volumetric force, $\theta_{I,J}$ a function of $\theta(\mathbf{X})$, \mathbf{X}_I and \mathbf{X}_J , with $\xi(\mathbf{X})$ and $\theta(\mathbf{X})$ blending functions satisfying $\xi(\mathbf{X}) + \theta(\mathbf{X}) = 1$.

To apply the displacement constraints between the continuum and atomistic descriptions in the interface, we use the Augmented Lagrangian method where we add a penalty term to the equation of the potential energy in addition to the Lagrange multipliers for the constraints as follows:

$$W_{AL} = W^{int} - W^{ext} + \boldsymbol{\lambda}^T \cdot \mathbf{g} + \frac{1}{2} p \mathbf{g}^T \cdot \mathbf{g} \quad (3)$$

with $\boldsymbol{\lambda} = \{\lambda_I\}$ a vector of Lagrange multipliers, $\mathbf{g} = \{g_I\}$ the constraints equation vector, and p a penalty parameter. In addition, we use a basis of shape functions (similar to what is done in finite element methods) for the Lagrange multipliers.

In this work, we implement a 1-D linear elasticity/linear spring model with linear constraints.

3. Model analysis

We analyze the model performance in terms of the error of the AtC model in relation to the full atomistic one, and compare it with a pure continuum model. In particular, we investigate the model sensitivity on the following components

1. Lagrange multiplier grid properties: Uniformity and resolution.
2. Finite element grid resolution.
3. Penalty parameter value.
4. Blending functions choice in the interface.
5. Lagrange multiplier basis functions choice.
6. Pairwise atomistic blending function $(\theta_{I,J})$ form.

This research implements different blending models, and deals with potential problems arising in the bridging region. In particular, we investigate the correct contributions of the continuum and atomistic expressions to the forces on the particles of the system.

4. Multiple-neighbor interaction

As an approach to long range interactions we implement a multiple-neighbor interaction, while keeping the linearity of the interaction type. Because we request each particle to interact with several neighbors, we need to apply the interaction in such a way that it will remain consistent with the same PDE applied to the continuum region used in the one-neighbor interaction. The equation of equilibrium of forces, for generalized number of neighbor interactions, has the following form:

$$-\sum_{\substack{\beta = \alpha - N_{neig} \\ \beta \neq \alpha}}^{\alpha + N_{neig}} \frac{\tilde{K}_{a,|\beta-\alpha|}}{|x_\alpha - x_\beta|} (d_\beta - d_\alpha) = f_\alpha^{ext} \quad (4)$$

with $\tilde{K}_{a,|\beta-\alpha|}/|x_\alpha - x_\beta|$ the linear spring force constant for the interaction between the particles α and β , and N_{neig} the number of neighbor interactions. We implemented two approaches:

1. Uniform force constant: $\tilde{K}_{a,|\beta-\alpha|} = \frac{2K_a}{N_{neig}(N_{neig}+1)}$
2. Non-uniform force constant: $\tilde{K}_{a,|\beta-\alpha|} = \frac{K_a}{|\beta-\alpha|N_{neig}}$

In order to check the error behavior of the multiple-neighbor AtC model in relation to the pure atomistic case, we isolate the boundary effects by implementing a “cheating method” combined with a “ghost atoms” boundary treatment, i.e. we assume that atoms near the boundary interact with “ghost atoms” beyond the boundary, while giving the “ghost” atoms the exact solution for their displacements as boundary conditions. We found that the non-uniform force constant choice gives smaller errors in the case of a constant load applied to the system.

As part of the multiple-neighbor interaction implementation, we need to apply a boundary treatment for those particles close to the boundary, which are not surrounded by enough particles. Generally speaking, if we change the number of neighbor interactions (N_{neig}), the value of the force constant changes accordingly (as presented above). In the following, we present different approaches we implemented for the boundary of the atomistic region:

1. Truncation: We assume an interaction with N_{neig} neighbors to the left and to the right, but truncate the interaction for atoms beyond the boundary.
2. Asymmetry: We use a different number of neighbor interactions to the left and to the right, using the maximum number of neighbors available (up to N_{neig}) inside the domain.
3. Adaptive: We use the same number of neighbor interactions to the left and to the right, using the maximum number of neighbors available (up to N_{neig}) inside the domain.
4. Extended Boundary Conditions: We extend the boundary conditions inside the domain to the first N_{neig} atoms closer to the boundary, and use N_{neig} neighbor interactions for the rest.
5. Ghost Atoms: We add “ghost atoms” beyond the boundary, having the same boundary conditions as the boundary atoms. The atoms inside the domain have N_{neig} neighbor interactions.

We found that the *adaptive* technique gives the best result, but it is not applicable to a general interaction form, thus the *ghost atoms* seems to be a good alternative.

5. Conclusions

We have presented an Atomistic to Continuum coupling approach where different models are coupled at the energy level, and the constraints are introduced through Lagrange Multipliers. The performance of the model is studied as a function of different parameters of the model. In particular, multiple neighbor interaction approaches with corresponding boundary treatments are presented.

Acknowledgments

We would like to thank Anter El-Azab for valuable discussions about continuum mechanics and Michael Parks for his comments about boundary treatments in the atomistic region.

References

- [1] S. Badia, P. Bochev, R. Lehoucq, M. L. Parks, J. Fish, M. A. Nuggehally, and M. Gunzburger. A Force-Based Blending Model for Atomistic-to-Continuum Coupling. *International Journal for Multiscale Computational Engineering*, 5:387–406, 2007.
- [2] J. Fish, M. A. Nuggehally, M. S. Shephard, C. R. Picu, S. Badia, M. L. Parks, and M. Gunzburger. Concurrent AtC coupling based on a blend of the continuum stress and the atomistic force. *Computer Methods in Applied Mechanics and Engineering*, 196:4548–4560, 2007.
- [3] T. Belytschko and S. P. Xiao. Coupling Methods for Continuum Model with Molecular Model. *International Journal for Multiscale Computational Engineering*, 1:115–126, 2003.

Effect of Thermal Cycling on Hardness of Plain Carbon Steel

Abdmanam Elmaryami

**The Higher Institute Of Mechanical Engineering, 218 Derna, Libya;
damer604@yahoo.com**

ABSTRACT

Thermal cycling tests were carried out on carbon steel up to 1.05 C% . A single run was performed at upper temperature of 500C⁰ and lower temperature of 30C⁰ in different media (water, sea water, and oil) . For several numbers of cycles up to 30 cycles for an accurate determination of heating and cooling times. The effect of thermal cycling on the hardness were evaluated, from the obtained test results, it was found that the hardness decreased without increasing the thermal cycling for both the annealed and tempered but this decreased in hardness very small and can be neglected.

Electronic Structure calculations of Novel Spinel Oxynitrides

Onyekwelu U. Okeke

Wits University, Johannesburg
Onyekwelu.Okeke@students.wits.ac.za

ABSTRACT

A spinel structure of an oxynitride material in the form M_3NO_3 (M=B, Al, Ga or In) is considered as being derived from a reaction of the form $M_2O_3 + MN \rightarrow M_3NO_3$. Various possible phases of MN and M_3O_3 are considered that could lead to the M_3NO_3 spinel material. The spinels containing B and Al exhibit higher resistance to compression and shear than those containing Ga and In and these are suggested to be potentially important hard materials possibly formed under extreme conditions. Calculated energetics of the proposed reaction favor the formation of the spinels containing Ga and In with such materials having potentially significant optoelectronic applications.

The Attainability of Hashin-Shtrikman Bounds

Liping Liu

¹ Division of Engineering and Applied Science, California Institute of Technology, Pasadena, CA 91125; liuliping@caltech.edu.

ABSTRACT

We discuss the attainability of the Hashin-Shtrikman (HS) bounds for multiphase composites, including those of conductive materials and elastic materials. A necessary and sufficient condition is obtained on the microstructures attaining these bounds. This condition provides a simple characterization of the attaining microstructures in terms of gradient Young measure, which enables us to attack the problem whether the HS bounds are attainable by the standard method in microstructure theory.

1. Introduction

One of the central problems in the theory of composites is to find the optimal bounds on the effective properties with or without restriction on the volume fraction, and if possible, to characterize all the microstructures that attain these optimal bounds ([1]). Among the most important bounds ([2], [1]), the Hashin-Shtrikman (HS) bounds appear ubiquitous for their simplicity and the perfect symmetry between the upper and lower bounds. It is now well known that the HS bounds describe the G_θ -closure of two-phase well-ordered conductive composites ([3], [1]), and that the HS bounds are insufficient to describe the G_θ -closure of composites of three or more phases ([4]). In the latter situation, the HS bounds may or may not be attainable. We study the conditions under which the HS bounds become attainable (resp. non-attainable) and how the attainable (resp. non-attainable) HS bounds depend on the volume fractions and material properties. This is the key problem we are going to address here. To this end, we begin with a novel derivation of the HS bounds for multiphase composites. The advantage of this new derivation is that it yields the attainment condition very naturally. In terms of a simple potential problem, the main condition is that the second gradient of the solution of the potential problem remains constant in all but the matrix phases. Further, using the concept of gradient Young measure ([5]), we obtain a simple and complete characterization of all the attaining microstructures of the HS bounds. From the basic relation between gradient Young measures and quasiconvex functions ([5]), we can then attack the problem by the standard approach in microstructure theory: we construct concrete microstructures to find the attainable HS bounds, and use quasiconvex functions to restrict the microstructures and find the non-attainable HS bounds. Below we present an outline of our arguments and main results. The details of them can be found in ([6]).

2. Hashin-Shtrikman bounds and their attainment conditions

To setup the problem, we consider a periodic $(N + 1)$ -phase composites in n -dimensional space of phases $\mathbf{L}_0, \dots, \mathbf{L}_N$, where $\mathbf{L}_i : \mathbb{R}^{n \times n} \rightarrow \mathbb{R}^{n \times n}$, symmetric and positive semi-definite (positive definite if restricted to $\mathbb{R}_{sym}^{n \times n}$), is the fourth-order tensor describing the material properties of phase- i for $i = 0, \dots, N$. Let $Y = (0, 1)^n$ be the unit cell of the periodic composite, $\Omega_i \subset Y$ be the regions occupied by phase- i and $\theta_i = vol(\Omega_i)$ be the volume fraction of phase- i for $i = 0, \dots, N$. By definition, the effective tensor \mathbf{L}^e of the composite is given by (see [1]),

$$\mathbf{F} \cdot \mathbf{L}^e \mathbf{F} = \min_{\mathbf{u} \in W_{per}^{1,2}(Y, \mathbb{R}^m)} \int_Y (\nabla \mathbf{u} + \mathbf{F}) \cdot \mathbf{L}(\mathbf{x})(\nabla \mathbf{u} + \mathbf{F}), \quad (1)$$

where $\mathbf{L}(\mathbf{x})$ takes value of \mathbf{L}_i if $\mathbf{x} \in \Omega_i$ and \mathbf{F} is an arbitrary $n \times n$ constant matrix. Since the equation $\text{Tr}(\nabla \mathbf{u}) = f$ admits a solution $\mathbf{u} \in W_{per}^{1,2}(Y, \mathbb{R}^m)$ for any given $f \in L^2_{per}(Y)$ with $\int_Y f = 0$, equation (1) can be rewritten as

$$\mathbf{F} \cdot \mathbf{L}^e \mathbf{F} = \min_{\substack{f \in L^2_{per}(Y) \\ \int_Y f = 0}} \min_{\substack{\mathbf{u} \in W_{per}^{1,2}(Y, \mathbb{R}^m) \\ \text{Tr}(\nabla \mathbf{u}) = f}} \int_Y (\nabla \mathbf{u} + \mathbf{F}) \cdot \mathbf{L}(\mathbf{x})(\nabla \mathbf{u} + \mathbf{F}). \quad (2)$$

To derive the lower and upper bounds for the effective tensor we assume the tensor \mathbf{L}_0 of phase-0, the so-called matrix phase, can be written as

$$(\mathbf{L}_0)_{piqj} = \mu_1 \delta_{ij} \delta_{pq} + \mu_2 \delta_{pj} \delta_{iq} + \lambda \delta_{ip} \delta_{jq}, \quad (3)$$

where $\mu_1 \geq \mu_2$, $\mu_1 + \mu_2 > 0$, and $\lambda > -\frac{\mu_1 + \mu_2}{n}$. The above form of tensors is convenient since it covers both cases of elasticity and conductivity. For simplicity, we assume $\mathbf{L}_i - \mathbf{L}_0$ is invertible restricted to $\mathbb{R}_{sym}^{n \times n}$ for all $i = 1, \dots, N$. Further, we write $\mathbf{L}_i \geq \mathbf{L}_0$ (resp. $\mathbf{L}_i \leq \mathbf{L}_0$) if $\mathbf{L}_i - \mathbf{L}_0$ is positive semi-definite (resp. negative semi-definite) and let

$$\Delta c_i = \mathbf{I} \cdot (\mathbf{L}_i - \mathbf{L}_0)^{-1} \mathbf{I}, \quad k_0 = \mu_1 + \mu_2 + \lambda, \quad \gamma = \sum_{i=0}^N \frac{\theta_i}{1/k_0 + \Delta c_i}, \quad \Delta c_* = \frac{1}{\gamma} - \frac{1}{k_0}. \quad (4)$$

For the lower bound, we assume that $\mathbf{L}_i \geq \mathbf{L}_0$ for all $i = 1, \dots, N$ and hence

$$(X + \mathbf{F}) \cdot (\mathbf{L}_i - \mathbf{L}_0)(X + \mathbf{F}) \geq \frac{1}{\Delta c_i} \text{Tr}(X + \mathbf{F})^2 \quad \forall i = 1, \dots, N \ \& \ X \in \mathbb{R}^{n \times n}. \quad (5)$$

Therefore, the inner minimum of the r.h.s. of Eqn (2) can be bounded from below as

$$\begin{aligned} \min_{\substack{\mathbf{u} \in W_{per}^{1,2}(Y, \mathbb{R}^m) \\ \text{Tr}(\nabla \mathbf{u}) = f}} \int_Y \{ (\nabla \mathbf{u} + \mathbf{F}) \cdot [\mathbf{L}(\mathbf{x}) - \mathbf{L}_0](\nabla \mathbf{u} + \mathbf{F}) + (\nabla \mathbf{u} + \mathbf{F}) \cdot \mathbf{L}_0(\nabla \mathbf{u} + \mathbf{F}) \} \\ \geq \sum_{i=1}^N \int_{\Omega_i} \frac{1}{\Delta c_i} (f + \text{Tr}(\mathbf{F}))^2 + k_0 \int_Y f^2 + \mathbf{F} \cdot \mathbf{L}_0 \mathbf{F}, \end{aligned} \quad (6)$$

where we have used

$$\int_Y \nabla \mathbf{u} \cdot \mathbf{L}_0 \nabla \mathbf{u} = \int_Y \left[\mu_1 |\nabla \mathbf{u}|^2 + \mu_2 \text{Tr}[(\nabla \mathbf{u})^2] + \lambda \text{Tr}(\nabla \mathbf{u})^2 \right] \geq k_0 \int_Y \text{Tr}(\nabla \mathbf{u})^2.$$

The above inequality can be easily shown by Fourier analysis. Similarly, for the upper bound, we assume that $\mathbf{L}_i \leq \mathbf{L}_0$ for all $i = 1, \dots, N$ and hence Eqn (5) holds with “ \geq ” replaced by “ \leq ”. Therefore, the inner minimum of the r.h.s. of Eqn (2) can be bounded from above as

$$\begin{aligned} & \min_{\substack{\mathbf{u} \in W_{per}^{1,2}(Y, \mathbb{R}^m) \\ \text{Tr}(\nabla \mathbf{u}) = f}} \int_Y \dots \leq \min_{\substack{\xi \in W_{per}^{2,2}(Y) \\ \text{Tr}(\nabla \nabla \xi) = f}} \int_Y (\nabla \nabla \xi + \mathbf{F}) \cdot \mathbf{L}(\mathbf{x}) (\nabla \nabla \xi + \mathbf{F}) \\ & \leq \min_{\substack{\xi \in W_{per}^{2,2}(Y) \\ \text{Tr}(\nabla \nabla \xi) = f}} \int_Y \left\{ (\nabla \nabla \xi + \mathbf{F}) \cdot [\mathbf{L}(\mathbf{x}) - \mathbf{L}_0] (\nabla \nabla \xi + \mathbf{F}) + (\nabla \nabla \xi + \mathbf{F}) \cdot \mathbf{L}_0 (\nabla \nabla \xi + \mathbf{F}) \right\} \\ & \leq \sum_{i=1}^N \int_{\Omega_i} \frac{1}{\Delta c_i} (f + \text{Tr}(\mathbf{F}))^2 + k_0 \int_Y f^2 + \mathbf{F} \cdot \mathbf{L}_0 \mathbf{F}, \quad (7) \end{aligned}$$

Plugging Eqn (6) and Eqn (7) into Eqn (2) and solving the outer minimization problem, we arrive at

$$\begin{cases} \mathbf{F} \cdot \mathbf{L}^e \mathbf{F} \geq \mathbf{F} \cdot \mathbf{L}_0 \mathbf{F} + \text{Tr}(\mathbf{F})^2 / \Delta c_* & \text{if } \mathbf{L}_i \geq \mathbf{L}_0 \forall i = 1, \dots, N, \\ \mathbf{F} \cdot \mathbf{L}^e \mathbf{F} \leq \mathbf{F} \cdot \mathbf{L}_0 \mathbf{F} + \text{Tr}(\mathbf{F})^2 / \Delta c_* & \text{if } \mathbf{L}_i \leq \mathbf{L}_0 \forall i = 1, \dots, N, \end{cases} \quad (8)$$

which coincides with the classic HS bounds for multiphase composites (see [1]). If we track back our arguments, it is not hard to show that the inequalities in Eqn (8) hold as equalities if and only if the following overdetermined problem

$$\begin{cases} \Delta \xi = \sum_{i=0}^N p_i \chi_{\Omega_i} & \text{on } Y, \\ \nabla \nabla \xi = \mathbf{Q}_i & \text{on } \Omega_i, \quad i = 1, \dots, N, \end{cases} \quad (9)$$

admits a solution $\xi \in W_{per}^{2,2}(Y)$, where

$$\mathbf{Q}_i = \mathbf{F} - \text{Tr}(\mathbf{F}) \frac{(1 + k_0 \Delta c_*)}{\Delta c_* (1 + k_0 \Delta c_i)} (\mathbf{L}_i - \mathbf{L}_0)^{-1} \mathbf{I}, \quad p_i = \text{Tr}(\mathbf{Q}_i) \quad (i = 1, \dots, N), \quad (10)$$

and p_0 is such that $\sum_{i=0}^N \theta_i p_i = 0$. In terms of gradient Young measure ([5]), this necessary and sufficient condition can be rephrased as the following theorem.

Theorem. Consider $(N + 1)$ -phase composites specified as above. The effective tensor \mathbf{L}^e (cf. Eqn (1)) satisfies the HS bounds (8). Further, the inequalities in (8) hold as equalities if and only if there exists a gradient Young measure ν with zero center of mass satisfying

$$\nu = \sum_{i=1}^N \theta_i \delta_{\mathbf{Q}_i} + \theta_0 \mu \quad \text{and} \quad \text{supp } \mu \subset \{X \in \mathbb{R}_{sym}^{n \times n} : \text{Tr}(X) = p_0\}, \quad (11)$$

where $\delta_{\mathbf{Q}_i}$ denote the Dirac mass at \mathbf{Q}_i , μ is a probability measure, and matrices \mathbf{Q}_i and p_0 are as in Eqn (10).

3. New results on the attainable and non-attainable Hashin-Shtrikman bounds

The above theorem converts the problem whether the HS bounds are attainable into the problem whether a particular form of gradient Young measure exists. The latter problem is more generic since it asks whether certain gradient field exists and is independent of material properties. Indeed, it is the special gradient field, not the geometry or topology, that entails the optimality of a microstructure. Further, this Theorem facilitates the use of many tools from the established theory of microstructure (see [7]). For example, from the convex property of gradient Young measures (see [5]), we can show that if all matrices \mathbf{Q}_i ($i = 1, \dots, N$) are positive semi-definite or negative semi-definite, then the gradient Young measure ν in Eqn (11) exists. This result, by the above Theorem and Eqn (10), enable us to find parts of the attainable HS bounds (8). Also, using the quasiconvex functions ([8], [7]) we can find restrictions on the gradient Young measure ν in Eqn (11), which then implies the non-attainable parts of the HS bounds (8). In conclusion, we obtain a simple characterization of the attaining microstructures of the HS bounds in terms of gradient Young measure which facilitates the construction and restriction of the optimal microstructures.

The author gratefully acknowledges the financial support of the US Office of Naval Research through the MURI grant N00014-06-1-0730.

References

- [1] G. W. Milton. *The Theory of Composites*. Cambridge University Press, 2002.
- [2] L. Tartar. Estimation fines des coefficients homogeneises. In *Ennio de Giorgi's Colloquium* ed. P. Kree, pages 168–187, 1985.
- [3] Y. Grabovsky. The G -closure of two well-ordered anisotropic conductors. *Proc. Royal Society of Edinburgh*, 123A:423–432, 1993.
- [4] N. Albin, A. Cherkaev, and V. Nesi. Multiphase laminates of extremal effective conductivity in two dimensions. *J. Mech. Phys. Solids*, 55:1513–1553, 2007.
- [5] D. Kinderlehrer and P. Pedregal. Characterization of Young measures generated by gradients. *Arch. Rational Mech. Anal.*, 115:329–367, 1991.
- [6] L. P. Liu. Hashin-shtrikman bounds for multiphase composites and their attainability. submitted to *Arch. Rational Mech. Anal.*, 2008.
- [7] J. Ball and R. D. James. *Mathematical Theory of Microstructure, manuscript*. 1997.
- [8] V. Šverák. New examples of quasiconvex functions. *Arch. Rational Mech. Anal.*, 119:293–300, 1992.

New Approach To Model Point Defects Migration Using A Monte-Carlo Paradigm Coupled With Artificial Intelligence

N. Castin¹, L. Malerba²

¹**Physique des Solides Irradiés et des Nanostructures (PSIN), Université Libre de Bruxelles (ULB), boulevard du Triomphe CP234, 1050 Brussels, Belgium.**

^{1,2}**SCK•CEN, Nuclear Materials Science Institute, Boeretang 200, B-2400 Mol, Belgium. (ncastin@sckcen.be ; lmalerba@sckcen.be)**

ABSTRACT

In this work, we propose to construct an Atomistic Kinetic Monte Carlo paradigm where the point defects migration barriers are calculated with few approximations on the basis of a Molecular Dynamics (MD) based method. The algorithm is speeded up with an Artificial Neural Network, trained to reproduce the migration barriers on the basis of the Local Atomic Environment, thus avoiding the need of an on-the-fly use of MD.

1. Introduction

It is widely accepted that the formation of copper-rich precipitates plays a key role in nuclear reactor pressure vessel steel hardening and embrittlement [1]. With this respect, any method capable of predicting the evolution of solute atom precipitation versus radiation dose helps at designing or monitoring nuclear reactor components (see e.g. [2][3]).

The Atomistic Kinetic Monte Carlo (AKMC) simulation [4] is a compromise between Molecular Dynamics (MD), which considers events at the atomic time and length scale, and coarse-grained tools, such as Object KMC [5] and rate theory [6], that are necessary to extend the simulation to the macroscopic scale. AKMC techniques retain the atomic level description, but reduce the number of possible events to the very basic mechanisms of single-defect diffusion and can thus encompass a timeframe (much) larger than MD.

In the AKMC algorithm, the events are vacancies and/or interstitials migration at a close neighboring position. The probabilities are calculated with the eqn. (1), where $\nu_{0,j}$ is a prefactor (assumed to be constant as Debye's frequency in Fe), k_B is Boltzmann's constant, T is the absolute temperature and E_j is the Migration Energy (ME) at 0K. The index j denotes the event for which the probability is calculated. The summation over k in the denominator is over all possible events. When the event is chosen, the simulation time is incremented with a mean residence time algorithm.

$$P_j = \frac{v_{0,j} \exp(-E_j/k_B T)}{\sum_k v_{0,k} \exp(-E_k/k_B T)} \quad (1)$$

The ME's are therefore the only unknowns that must be calculated on the fly during the simulation, depending on the instantaneous Local Atomic Environment (LAC) of the migrating point defects. They are classically estimated with empirical formula based on the difference on energy induced by the migration, or numerically fitted on the basis of a limited amount of *ab initio* data.

It is clear that the ME quality (depending on the method used to calculate it) is strongly influencing the kinetic path followed by the system. Empirical formulas based on the energy difference have the advantage to be very easy to do on-the-fly, but give a poor description of the energy barriers, mainly because there are in reality very poorly correlated with the energy difference. On the other extremity, *ab initio* methods are unquestionably the state-of-the-art but can only provide a rather limited amount of calculations because of their inherent complexities.

2. Methodology

In our method, we propose to calculate the ME with an MD based tool. The Nudged Elastic Band (NEB) method [7] optimizes the Minimum Energy Path (MEP) of the migrating particle from the initial to the final state of the system (that are both relaxed with a conjugate gradients method), by constructing a chain-of-states linked with fictive springs. The saddle point in the MEP, corresponding to the ME, is found with a good accuracy. This method therefore provides an automated procedure to calculate the ME, entirely based on the inter-atomic potential used in an MD framework to calculate the total energy of the system.

The NEB method allows us to calculate any ME in a reasonable timeframe. As an order of magnitude, the calculation of the vacancy migration energy takes about 100 seconds on a modern mono-processor machine. This is, however, much too slow to envisage an on-the-fly use in the AKMC simulation. But the generation of considerably large databases of examples, corresponding to original LAC's, is possible.

Once large databases of NEB calculated examples have been generated, we train an Artificial Neural Network (ANN) to construct a mathematical regression between the LAC and the corresponding ME. The ANN input variables are categorical integers, describing the chemical nature of the neighboring atoms situated at fixed positions in a rigid lattice grid of coordinates. Our ANN is a Multi-Layer Perceptron with only one hidden layer, trained with a Levenberg-Marquardt algorithm [8]. Only a small part of the ME database is used as a training set, to adapt the degrees of freedom in the ANN. The rest is used as a validation set, to assess the ANN extrapolation qualities on never seen examples. Once trained, the ANN is by 6 to 7 orders of magnitude faster than NEB in providing an estimate of the ME.

3. Results

Figure 1 shows the ANN quality of predictions for a simple FeCu binary system, with only one vacancy. A database of more than 100,000 randomly generated examples has been NEB calculated. The ANN has been trained using only 15,000 of them, taking the third nearest neighbors of both the migrating atom and its destination into account (that makes 39 variables for a BCC crystallographic structure). The average ANN error measured on the rest of the database is of the same order as the estimated NEB accuracy. We can therefore consider that the use of an ANN, in this case, is fully equivalent than if NEB is used on the fly during an AKMC simulation.

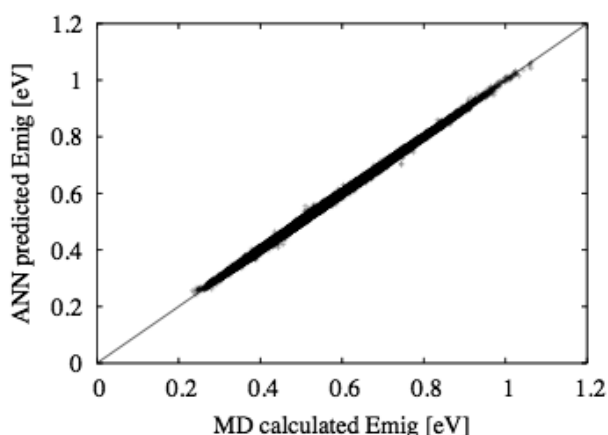


Figure 1 – ANN quality of prediction for the 1nn migration of a vacancy in an FeCu alloy. 39 atomic sites are taken into account. The average error is 0.51% and $R^2 = 0.999$. The points shown where not used for training.

The problem of Self-Interstitial Atom (SIA) migration is much more complicated than for vacancies, because of the strong and highly anisotropic interaction between close ones. We still have some problems to calculate their ME with a sufficient accuracy, because the relaxation of a small system containing several SIA's, with the constraint to keep their orientations and positions, can be a delicate issue. The problem is to guarantee that the migration path found by the NEB method gives truly the lowest possible saddle point energy for a given transition. Meanwhile, we have managed to train the ANN to predict the difference of (relaxed) energy for the 1nn migration of a $\langle 110 \rangle$ dumbbell, in pure Fe with maximum 4 other SIA's in the box, as shown on figure 2. 145 atomic sites were taken into account and 80,000 examples were used for training.

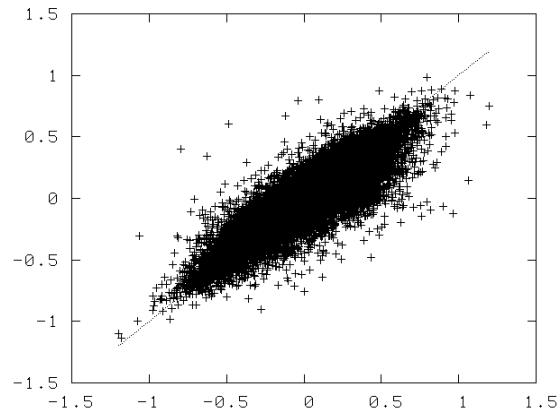


Figure 2 – ANN predictions of the relaxed energy difference for the 1nn migration of a $\langle 110 \rangle$ dumbbell in pure Fe. The X axis is the MD value, the Y axis is the ANN predicted. The average error is 0.07 eV and $R^2 = 0.89$.

Acknowledgements

This work was performed in the framework of the FP6 PERFECT project, partially funded by the European Commission under contract FI6O-CT-2003-508840.

References

- [1] G.R. Odette and G.E. Lucas, JOM 53 (7) (2001) 8-22. Mater. Sci. Eng. 6 (1998) 19-28.
- [2] K. Fukuya, K. Ohno, H. Nakata, S. Dumbill and J.M. Hyde, J. Nucl. Mater. 312 (2003) 163-173.
- [3] Y. Nagai, Z. Tang, M. Hasegawa, T. Kanai and M. Saneyasu, Phys. Rev. B 63 (2001) 134110.
- [4] B.D. Wirth and G.R. Odette, "Kinetic lattice Monte Carlo simulations of cascade aging in iron and dilute iron-copper alloys", Mat. Res. Soc. Symp. Proc. 540 (1999) 637-642.
- [5] C. Domain, C.S. Becquart and L. Malerba, J. Nucl. Mater. 335 (2004) 121.
- [6] C. Ortiz, M.-J. Caturla, C.-C. Fu and F. Willaime, Phys. Rev. B 75, 100102(R) (2007).
- [7] H. Jonsson and G. Mills and K. W. Jacobsen, "Nudged Elastic Band method for finding minimum energy paths of transitions", Classical and quantum dynamics in condensed phase simulations, B. J. Berne G. Ciccotti and D. F. Coker (World Scientific, Singapore), 1998.
- [8] C.M. Bishop, "Neural Networks for pattern recognition", Clarendon press, Oxford, 1995.

Regression Possibilities of Isothermal Transformation (IT) and Continuous Cooling (CC) Transformation Diagrams using T-t Elements

Zoltan Dudas

**Department of Materials Science and Engineering, BUTE, Budapest, Hungary
dudas@eik.bme.hu**

ABSTRACT

The first part of this document demonstrates developed numerical isothermal (IT) diagrams, which are built up by Temperature-time (T-t) elements, approximated from four measured base IT diagrams connected to two carbon contents and two austenitisation temperatures. The second part of this document demonstrates the developed numerical continuous cooling (CC) diagrams, which are built up also by Temperature-time (T-t) elements, approximated from four measured base CC diagrams connected to the same two chemical compositions and two austenitisation temperatures. The third part of the document shows the regression possibilities by creation of virtual IT diagrams from the numerical approximated base transformation diagrams for a third carbon content and two given austenitisation temperature, and shows the comparison between the calculated virtual diagram data and the measured data (characterised by the third carbon content and the applied austenitisation temperature at the measurement). The fourth part of the document shows the regression possibilities by creation of virtual CC diagrams from the numerical approximated base transformation diagrams for a third carbon content and two given austenitisation temperature, and shows the comparison between the calculated virtual diagram data and the measured ones (characterised by the third carbon content and the applied austenitisation temperature at the measurement).

Analytic Solution of the Discrete Double Sine-Gordon Model: application to crowdion migration in the bcc transition metals

Steve Fitzgerald , Duc Nguyen-Manh Zoltan Dudas

**EURATOM/UKAEA Fusion Association, Culham Science Centre, Abingdon, UK;
steve.fitzgerald@ukaea.org.uk, duc.nguyen@ukaea.org.uk**

ABSTRACT

We present the first derivation of the analytic solution for the crowdion migration potential which takes into account discreteness within the double sine-Gordon model. The analysis is guided by the group-specific trend in the shapes of the periodic substrate potentials calculated for the body-centred-cubic transition metals in groups 5B and 6B of the periodic table. We combine density-functional calculations of the crowdion's profile and environment with an extended version of the analytical Frenkel-Kontorova model, and determine the effective potential experienced by the defect's centre-of-mass. This reveals important underlying differences between these bcc metals, which are inaccessible to either the numerical or analytical approaches alone, and offers a clear explanation for the significantly higher crowdion migration temperatures observed in the metals of Group 6B. This work is supported by the UK Engineering and Physical Sciences Research Council and by EURATOM.

Generalisation of the Diffusion-Reaction Theory for Inclusion Of Complexes with Long-Range Interaction Range

**Alexander V. Barashev¹, Stanislav I. Golubov^{2,3}, David J. Bacon¹,
Yury N. Osetsky², Roger E. Stoller²**

¹**Department of Engineering, The University of Liverpool, Brownlow Hill, Liverpool, L69 3GH, UK , a.barashev@liv.ac.uk, djbacon@liv.ac.u**

²**Materials Science and Technology Division, ORNL, Oak Ridge, TN 37831- 6138, USA, 6gs@ornl.gov (S.I.G.) osetskiyyn@ornl.gov (Yu.N.O.), rkn@ornl.gov (R.E.S.)**

³**Center for Materials Processing, University of Tennessee, East Stadium Hall, Knoxville, TN 37996-0750, USA.**

ABSTRACT

Some lattice defects, such as phase precipitates and dislocations, have long-range interaction range with migrating species, hence spectrum of the interaction energy. The dissociation rate of such complexes is not a reciprocal of the mean dissociation time and this is due to non-exponential distribution of dissociation times. In this paper, for the first time, an equation for the dissociation rate and the rate equation for concentration of such complexes are derived. It is shown that the modifications to the conventional expression for the reaction rate are connected closely with action of a general principle that the slowest process in the system controls the evolution. Monte Carlo calculations for traps in the form of triangular and square potential wells are performed to compliment the analysis and verify the conclusions. The memory effects due to the non-exponential distribution are discussed in details. The results are believed to be of interest for a wide range of applications.

A.V.B. acknowledges a research grant from the UK Engineering and Physical Sciences Research Council. Research at ORNL was sponsored by the Division on Materials Sciences and Engineering (R.E.S. and Y.N.O.) and the Office of Fusion Energy Sciences (S.I.G.), U. S. Department of Energy, under contract no. DE-AC05-00OR22725 with UT-Battelle, LLC.